AALBORG UNIVERSITY
SCHOOL OF ENGINEERING AND SCIENCE

Nonlinear analysis of reinforcement effects on concrete elements

Master of Science Final Project

Lucian-Aurelian Ionita

Supervisor,
Johan Clausen, Associate Professor, PhD

June 8,2016

AALBORG UNIVERSITY
STUDENT REPORT

School of Engineering and Science
Department of Civil Engineering
Fibigerstraede 10
Telephone: 99 40 84 84
Fax: 99 40 85 52
http://www.civil.aau.dk/

Title:

Finite-element modelling of reinforced concrete

Project Period:

3rd and 4th Semester, Master's Program in Structural and Civil Engineering, 2015-2016

Members:

Lucian Ionita

Supervisor:

Johan Clausen

Issues: 3
Page Numbers: 71
Submission Date: 08.06.2016

Synopsis:

The project deals with the observation of the effect of reinforcement on a concrete element. The elements are analyzed with both analytic and numerical approach in order to see the effect of the reinforcement on the load bearing capacities and deformations.
The analytic determination of load bearing capacities and deformations are done with the help of a model based on the Eurocode Standard.
The numerical model will be done with the help of the software Abaqus.
A comparison of these two models and their results was made and a conclusion was carried out.

Preface

The present project is created by Lucian-Aurelian Ionita, student of the Master's Program in Structural and Civil Engineering at Aalborg University. The project title is "Finite element analysis of reinforced concrete" and it has been done by the course of 3rd and 4th semester.

Reading Guide

The report consist of an analytic and numerical analysis of concrete elements. The report is enclosed on the Appendix CD.

In the report the source references are listed as the Harvard-method whereby the text refers to [Surname, Year]. Books are listed with author, title, publisher, and year. Web addresses are stated with author, title, and date.

Figures and tables are numbered with reference to chapter and an explanatory text is shown below the figure and above the table. The report uses numbered equations where the numbering of the equations appears in parentheses and is placed in the right side of the document. The numbering of the equations is likewise by chapter.

Lucian-Aurelian Ionita

Contents

Introduction 1

The objective of the project is a structural analysis, analytic and numerical, of concrete elements with an uniform cross-section and simple geometry with and without reinforcement, and compare their results. In Figure 1.1 it is seen a plain beam and in Figure 1.2 it is seen a reinforced concrete beam.

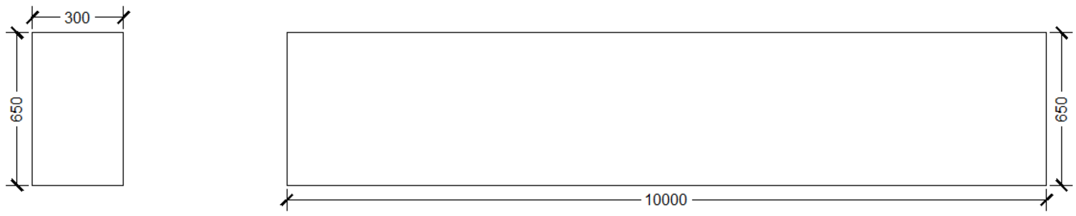

Figure 1.1. Example of concrete beam with no reinforcement.

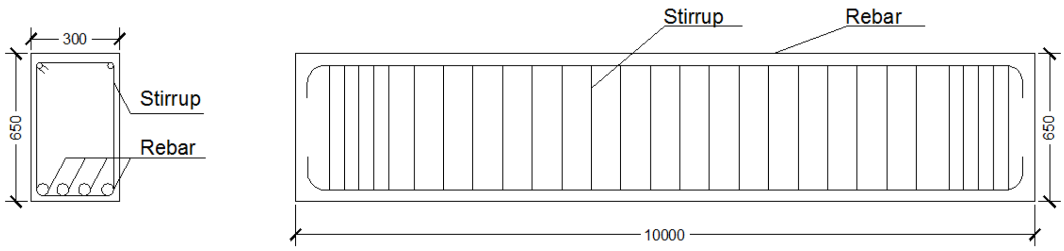

Figure 1.2. Example of concrete beam with rebar and stirrup reinforcement.

The main purpose is to see how different types of reinforcement affects the bearing capacity of the concrete elements. The analytic approach consists of calculating the strength of the beam according to the Eurocode standard and the numerical approach will be done by analyzing a model created with the software Abaqus. Because of the fact that concrete is a non-linear material the analytic calculations, which are based on linear properties of materials, will give an approximation of the real strengths. The numerical model is an advanced 3D model which takes into account the non-linearity of the concrete properties and it is expected to produce results closer to the behavior of the real concrete element. The concrete elements are assumed to be simply supported. In order to simplify the calculations a symmetry plane is used around the middle of the beam sectioning it in two identical halves as seen in Figure 1.3.

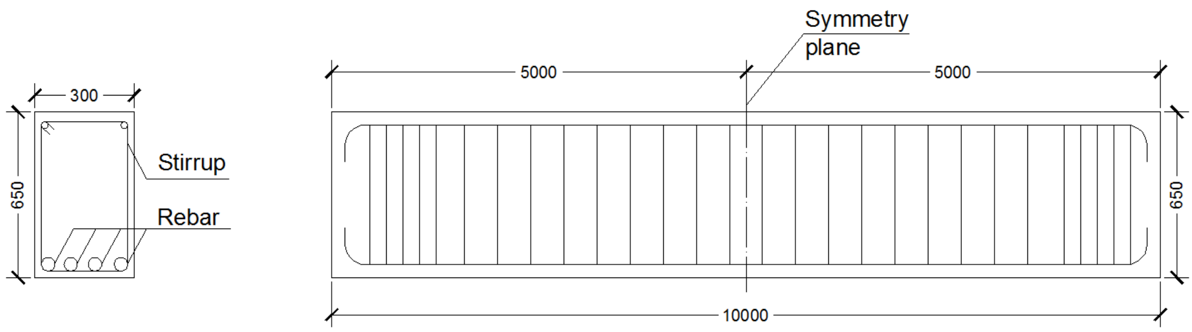

Figure 1.3. Symmetry plane around the center of the concrete beam.

1.1 Thesis Statement

The main thesis statement of the report is:
The observation of the influence that reinforcement has on the bearing capacities and deformations of concrete elements.

The bearing capacities are determined by analytic method with the help of the Eurocode. Then they are determined again with a numerical model created in a finite element analysis software. Reinforcement rebars are introduced in the calculations to see it's effect on the characteristic of the concrete element and a new analytic and numerical analysis are performed. Additionally, stirrups are added to the existing reinforcement in order to see their effects on load bearing capacity.

1.1.1 Assumptions and Limitations

Through the calculations and creation of the models different assumptions are made which are explained when used in each chapter. The limitations for the project are:

- Only simple cross-sections and geometries are analyzed.
- Simple type of reinforcement geometry used.
- Only one type of concrete class is being considered.
- No experiment is done to compare the analytic and numerical results with the real behavior of the concrete elements.

Materials 2

In this chapter the materials, and their properties, used in the report are presented.

2.1 Concrete

Concrete is one of the oldest building material known to man, being used as early as the Roman Empire. The modern concrete was created with the discovery of the Portland cement. It is mainly composed of four elements:

- Coarse aggregate
- Fine aggregate
- Portland cement
- Water

With new technology available, concrete can have its properties change with the help of special additives called admixtures, eg. speeding up the hardening, increasing the workability of fresh concrete, etc. It is a material which has a very high compression strength, but much lower tension strength. Concrete is a highly non-linear material which makes it difficult to model analytically or numerically without some assumptions which simplify its behavior. The linear-elastic behavior is observed in Figure 2.1, the linear-elastic perfectly plastic in Figure 2.2 and behavior of concrete in Figure 2.3.

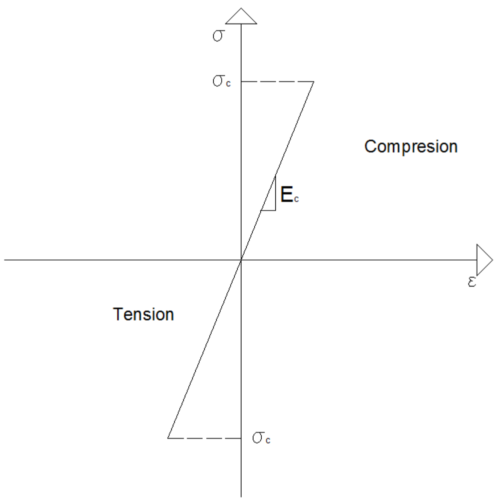

Figure 2.1. Linear-elastic stress-strain curve of material.

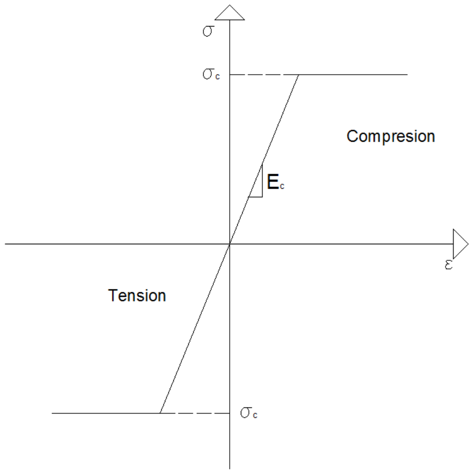

Figure 2.2. Linear-elastic perfectly plastic stress-strain curve of material.

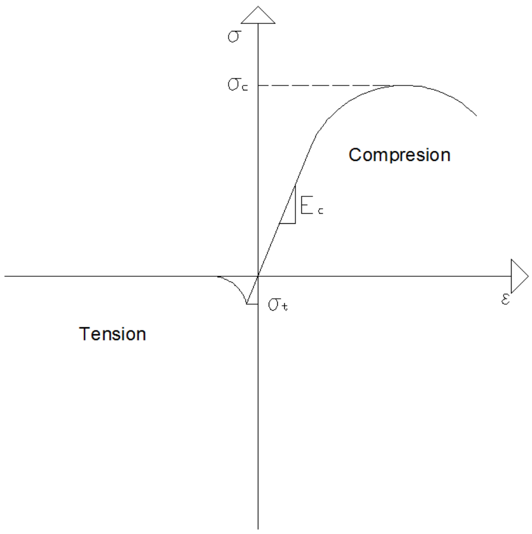

Figure 2.3. Stress-strain curve of concrete.

The concrete chosen for the models in this project has the class C20/25, which means that during testing of different specimens, the cylindrical specimen has a compression strength of $20\,\mathrm{N/mm^2}$ and the cube specimen has a compression strength of $25\,\mathrm{N/mm^2}$. According to [EN 1992-1-1, 2014], the tensile strength for this concrete class is $1.5\,\mathrm{N/mm^2}$ and its Young's modulus is $30\,000\,\mathrm{N/mm^2}$. All the numerical models won't have any assumptions so they will have the stress-strain curve seen in Figure 2.3.

2.2 Steel

Steel is an alloy of iron and other elements, mostly carbon, which is used as a construction material due to it's high tensile strength and low cost. Steel alone is prone to fire and corrosion and it's expensive to maintain, but it is used as reinforcement because the concrete offers protection against fire and corrosion. According to [Autodesk, 2015] the stress-strain curve is seen in Figure 2.4.

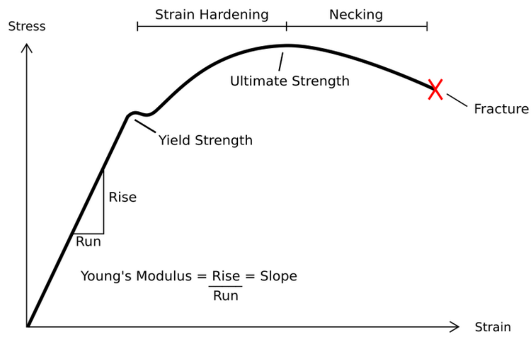

Figure 2.4. Stress-strain curve of a uniaxially loaded steel specimen, [Autodesk, 2015].

According to [EN 1992-1-1, 2014] for analytic calculations, an ideal stress-strain curve is used to show the behavior of steel as seen in Figure 2.5.

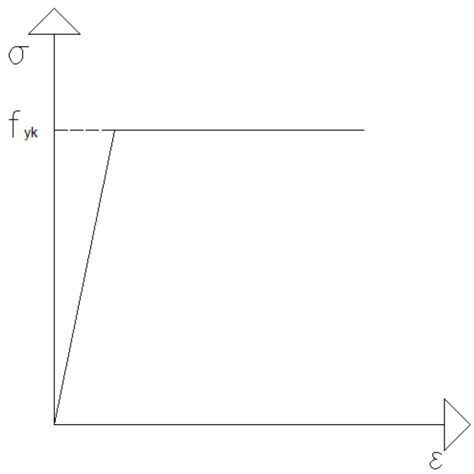

Figure 2.5. Idealized stress-strain curve of steel.

The type of steel used for reinforcement in the project is S275 Steel which has a yielding strength of 275 MPa and Young's modulus of $2.1 \times 10^5\ \mathrm{N/mm^2}$

Analytic Beam design 3

In this chapter an analytic approach is used in order to calculate the bearing capacity and maximum displacements of a 2D concrete beam due to an external load.

The analysis is performed based on calculation from the [EN 1992-1-1, 2014]. A plain concrete beam and a reinforced concrete beam are compared in terms of deformation and bearing capacity.

3.1 Plain concrete beam

3.1.1 Beam model

The analytic model is created such that it resembles the real model in order to be able to get accurate results. For the model a simply supported, statically determinate beam with a rectangular cross-section with a width of 300 mm and height of 650 mm and 10 000 mm long is used. It is considered to be loaded with an uniform load q. The static scheme and cross-sections of the beam is seen in Figure 3.1.

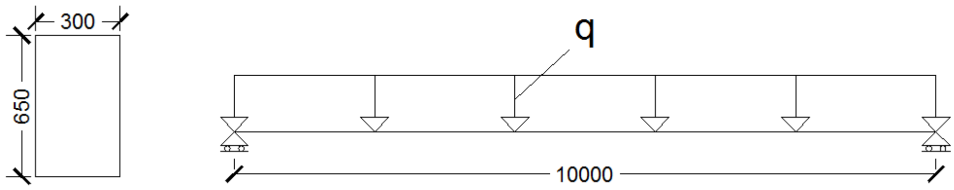

Figure 3.1. Static scheme and cross-section of the beam.

3.1.2 Load bearing capacity

In order to simplify the analytic analysis of the load bearing capacity, an assumption is made, it is considered that the concrete has a linear elastic behavior. It is assumed that the concrete reaches its characteristic strength. The stress distribution is seen in Figure 3.2.

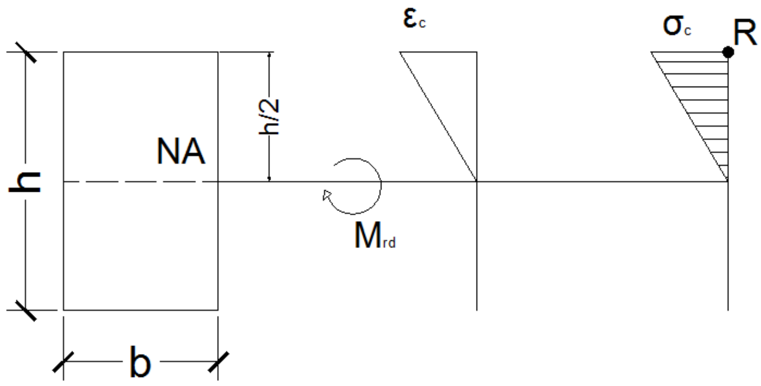

Figure 3.2. Stress distribution in the beam.

To find the moment capacity of the beam an equilibrium of moments is considered around point R. The moment capacity is found with Equation (3.1).

$$\begin{aligned}
&\sigma_c \cdot \frac{h}{2} \cdot b \cdot \frac{1}{3} \cdot \frac{1}{2} \cdot \frac{h}{2} - M_{rd} = 0 \\
&M_{rd} = \sigma_c \cdot \frac{h}{2} \cdot b \cdot \frac{1}{3} \cdot \frac{1}{2} \cdot \frac{h}{2}
\end{aligned} \tag{3.1}$$

Because it is assumed that the concrete reaches its characteristic strength the stresses in the concrete are assumed to be the characteristic strength so the previous equation becomes Equation (3.2).

$$M_{rd} = f_{ck} \cdot \frac{h}{2} \cdot b \cdot \frac{1}{3} \cdot \frac{1}{2} \cdot \frac{h}{2} \tag{3.2}$$

The resulting moment capacity is 1.05×10^8 Nmm. In order to transform the moment capacity in load bearing capacity, it is required to write the moment capacity in function of load bearing capacity so Equation (3.3) is used.

$$M_{rd} = q_{cap} \cdot \frac{L^2}{8} \tag{3.3}$$

M_{rd}	Moment capacity of the beam
q_{cap}	Load bearing capacity of the beam
L	Length of the beam

From this formula the load bearing capacity is isolated and its value is determined with Equation (3.4).

$$q_{cap} = 8 \cdot \frac{M_{rd}}{L^2} \tag{3.4}$$

The obtained load bearing capacity is 8.45 N/mm.

3.1.3 Deflections

By using the bearing capacity the maximum deflection can be calculated. For a beam loaded by an uniformly distributed load the maximum deflection are at the middle of the beam as it is seen in Figure 3.3.

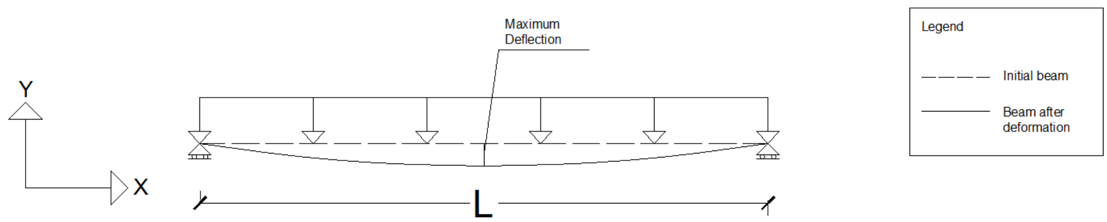

Figure 3.3. Maximum displacement for the beam.

According to [EN 1992-1-1, 2014] the maximum deflection allowed in a beam is given by Serviceability Limit State and has the Equation (3.5).

$$\delta_{max} = \frac{L}{250} \tag{3.5}$$

δ_{max}	Maximum allowed displacement
L	Initial span of beam

The maximum allowed deflection is 40 mm.

To calculate the maximum displacement in the beam Equation (3.6) is used. In order for this equation to be true, the concrete is assumed to act linear-elastic.

$$\delta = \frac{5}{384} \cdot \frac{q_{cap} \cdot L^4}{E \cdot I} \tag{3.6}$$

δ	Displacement at half span
q_{cap}	Load bearing capacity
L	Span of beam
E	Young's Modulus
I	Moment of inertia

The elastic modulus is different for each type of concrete class. For the calculation Concrete class 20 is chosen and its Elastic modulus according to Table 11.3.1 from [EN 1992-1-1, 2014] is $30\,000\,\mathrm{N/mm^2}$. The moment of inertia depends on the cross-section of the beam and is calculated with Equation (3.7).

$$I = \frac{b \cdot h^3}{12} \tag{3.7}$$

I	Moment of inertia
b	Width of beam
h	Height of beam

The obtained moment of moment of inertia is $6.87 \times 10^9\,\mathrm{mm^4}$. The displacement in the middle of the beam is 5.52 mm which is less than the maximum allowed displacement of 40 mm, meaning that the Serviceability Limit State equation is satisfied.

3.2 Reinforced concrete beam

A plain concrete beam is rarely suitable for construction of a building as it has a low bearing capacity so reinforcement is added to the beam in order to increase the bearing capacity. The reinforcement used for the beam can vary depending on the type of building constructed, its importance to society, etc.

3.2.1 Beam model

During its life a beam is mostly subjected to bending which cause the beam to deflect in such a way that it has a compressed zone and a tensed zone as seen in Figure 3.4.

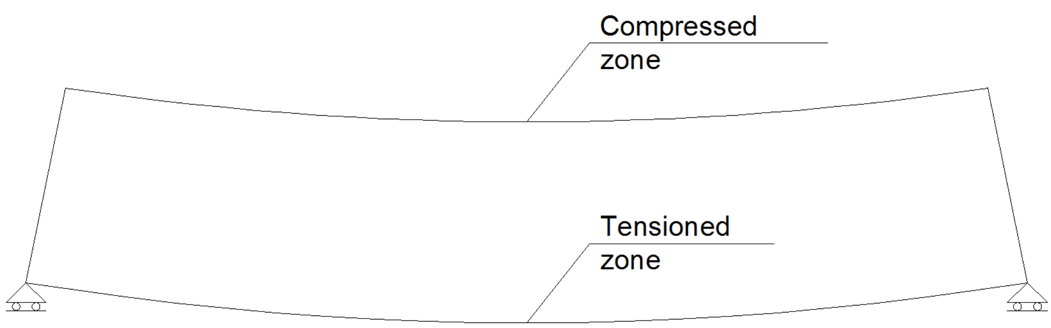

Figure 3.4. Compressed and tensioned parts of the beam.

It is well known that concrete is a material that has a very good compression resistance but acts poorly in tension so reinforcement is introduced in the tensioned part in order to take the tensile stresses the beam is subjected to and to increase the bearing capacity of the beam. In some occasions reinforcement is also used in the compressed part in order to further increase the bearing capacity or for constructive reasons, such as being supports for stirrups. For example in case a load which would make the building vibrate, eg. an earthquake, the beam will continously alternate the two zones during the time the load is acting on the structure as seen in Figure 3.5.

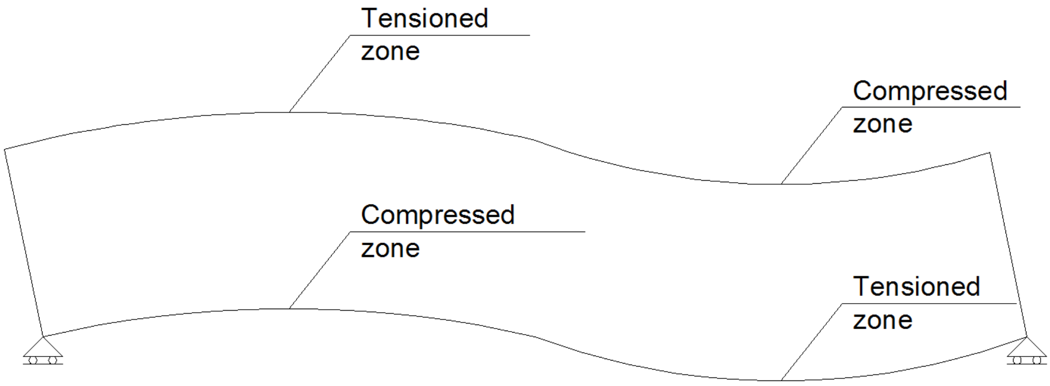

Figure 3.5. Compressed and tensioned parts of the beam during and earthquake.

In this case the reinforcement at the top of the beam is as important as the one at the bottom.

The beam analyzed in the project is considered to never be acted by an earthquake load so only the bottom reinforcement will be calculated and the top reinforcement will only be considered for constructive reasons. The cross section beam is seen in Figure 3.6.

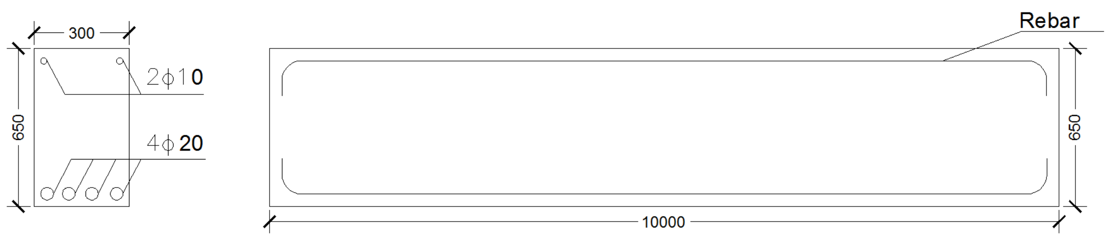

Figure 3.6. Reinforced concrete beam cross section.

As the tensioned zone is the important one, the rebars at the bottom of the beam need to be stronger so a higher diameter of the rebar is chosen, while at the top of the beam a smaller diameter of the rebar is chosen. The bottom reinforcement will consist of four ϕ 20 and the top reinforcement will consist of two ϕ 10 as seen in Figure 3.7.

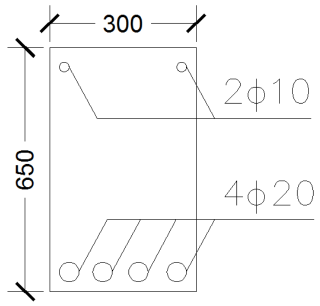

Figure 3.7. Reinforced concrete beam cross section.

3.2.2 Materials

A reinforced concrete beam is a composite beam made of concrete and steel. It is considered composite as the materials are behaving simultaneously when a force acts on it.

Steel

Steel is a material which has a very good tensile strength, hence why it is used as reinforcement for the tensioned part of the concrete. The properties of steel are presented in Chapter 2.

Concrete

The properties of concrete are presented in Chapter 2. Because the concrete has low tensile strength, steel reinforcement bars are used in order to increase it's strength.

3.2.3 Load Bearing Capacity

In order to be able to do analytic calculations an assumption of the real behavior of concrete is done. It is considered that the concrete has a linear elastic behavior. This doesn't reflect the real behavior of the concrete and the assumption is done in order to simplify the calculations. All the dimensions required for the computation of the stresses, strains and deflection are shown in Figure 3.8.

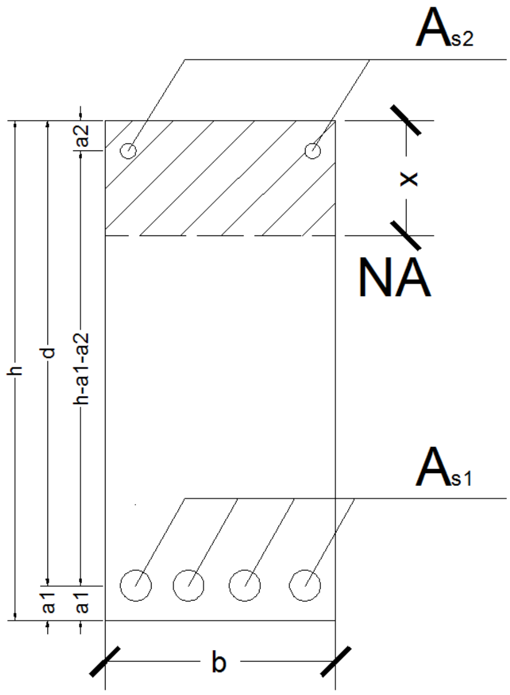

Figure 3.8. Dimensions of the beam cross-section.

b	Width of beam
h	Height of beam
$a1$	Concrete cover for the bottom reinforcement
$a2$	Concrete cover for the top reinforcement
d	Effective height of the cross section
$As1$	Area of bottom reinforcement
$As2$	Area of top reinforcement
x	Compressed zone
NA	Neutral Axis

There are two ways of calculation the bearing capacity of the beam depending on how we consider the behavior of the concrete and reinforcement.

Linear Elastic Approach

The bearing capacity of the beam is calculated assuming that the stresses in the concrete reach its characteristic strength. The stress distribution is seen in Figure 3.9.

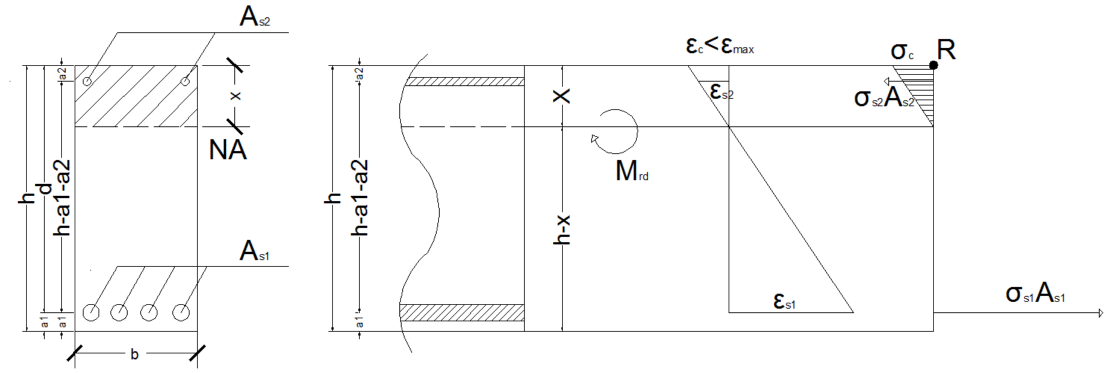

Figure 3.9. Assumed stress-strain of concrete.

σ_c	Stress in concrete
σ_{s1}	Stress in the bottom reinforcement
σ_{s2}	Stress in the top reinforcement
ϵ_c	Strain in concrete
ϵ_{s1}	Strain in the bottom reinforcement
ϵ_{s2}	Strain in the top reinforcement
M_{rd}	Resistive bending moment

The initial limit state equations used in calculations are the following:

$$\sigma_c = \epsilon_c \cdot E_c = f_{ck} \tag{3.8}$$

$$\sigma_{s1} = \epsilon_{s1} \cdot E_s \leq f_{yk} \tag{3.9}$$

$$\sigma_{s2} = \epsilon_{s2} \cdot E_s \leq f_{yk} \tag{3.10}$$

E_c	Young's modulus of concrete
E_s	Young's modulus of steel
f_{ck}	Characteristic strength of concrete
f_{yk}	Characteristic strength of steel

In the project it is considered that the reinforcement starts to yield before the concrete fails and concrete fails before the bars fail so by using the aforementioned equations we limit the maximum stress in the concrete but not in the reinforcement. In this case the stresses in the bottom rebars are $402\,\mathrm{N/mm^2}$ and the top stresses in the top rebars are $113\,\mathrm{N/mm^2}$, which means that the bottom rebars fail before the concrete fails so the consideration is wrong. In order to correct this the stresses in the bottom bars are limited to the yielding stress and new values for the strains and stresses are calculated.

By using the new values, the new recalculated stresses and strains are smaller than the ones before. The new stresses in the top bars are $77.64\,\mathrm{N/mm^2}$.

In order to find the compressed zone of the beam, which is the only part of the beam in which concrete has strength, an equilibrium equation on the horizontal direction is used. The equilibrium equation is Equation (3.11).

$$\sigma_{s1} \cdot A_{s1} - \sigma_{s2} \cdot A_{s2} - \sigma_c \cdot x \cdot \frac{1}{2} \cdot b = 0 \tag{3.11}$$

Equations (3.8), (3.9) and (3.10) are introduced in Equation (3.11) so a new equation is formed which is Equation (3.12).

$$\epsilon_{s1} \cdot E_s \cdot A_{s1} - \epsilon_{s2} \cdot E_s \cdot A_{s2} - f_{ck} \cdot x \cdot \frac{1}{2} \cdot b = 0 \tag{3.12}$$

Because of the new limit state equations the strains have to also be recalculated, this is done in order to be sure that the strains do not exceed the limits. The new strains are found with Equations (3.13) and (3.14).

$$\frac{\epsilon_c}{\epsilon_{s1}} = \frac{x}{h - x - a_1} \Rightarrow \epsilon_{s1} = \frac{\epsilon_c \cdot (h - x - a_1)}{x} \tag{3.13}$$

$$\frac{\epsilon_c}{\epsilon_{s2}} = \frac{x}{x - a_2} \Rightarrow \epsilon_{s2} = \frac{\epsilon_c \cdot (x - a_2)}{x} \tag{3.14}$$

By introducing Equations (3.13) and (3.14) in Equation (3.12) a new equation in function of x is obtained. The obtained formula is Equation (3.15).

$$\frac{\epsilon_c \cdot (h - x - a_1)}{x} \cdot E_s \cdot A_{s1} - \frac{\epsilon_c \cdot (x - a_2)}{x} \cdot E_s \cdot A_s 2 - f_{ck} \cdot x \cdot \frac{1}{2} \cdot b = 0 \tag{3.15}$$

Solving x from this equation the height of the compressed part of the beam is found out. The obtained height is 162.7 mm

In order to find the bearing capacity of the beam an equilibrium of moments is considered around point R. The moment capacity is found with Equation (3.16).

$$\begin{gathered} \frac{1}{3} \cdot \sigma_c \cdot x \cdot \frac{1}{2} \cdot b + a_2 \cdot \sigma_{s2} \cdot A_{s2} - (h - a_1) \cdot \sigma_{s1} \cdot A_{s1} - M_{rd} = 0 \\ M_{rd} = \frac{1}{3} \cdot \sigma_c \cdot x \cdot \frac{1}{2} \cdot b + a_2 \cdot \sigma_{s2} \cdot A_{s2} - (h - a_1) \cdot \sigma_{s1} \cdot A_{s1} \end{gathered} \tag{3.16}$$

The resulting moment capacity is 1.85×10^8 N $\times$ mm. In order to transform the moment capacity in load bearing capacity, it is required to write the moment capacity in function of load bearing capacity so Equation (3.17) is used.

$$M_{rd} = q_{pl} \cdot \frac{L^2}{8} \tag{3.17}$$

M_{rd}	Moment capacity of the beam
q_{pl}	Load bearing capacity of the beam
L	Length of the beam

From this formula the load bearing capacity is isolated and its value is determined with Equation (3.18).

$$q_{pl} = 8 \cdot \frac{M_{rd}}{L^2} \tag{3.18}$$

The obtained load bearing capacity is 14.85 N/mm.

Fully Plastic Approach

In this approach it is assumed that concrete reaches full plasticity and the rebars reach their yielding stress. According to [EN 1992-1-1, 2014] the stress distribution in the concrete in real life is parabolic but in order to simplify it for the calculations it is assumed to be a rectangular distribution which has the area as 80 % the area under the curve of the parabola as seen in Figure 3.10 and Equation (3.19).

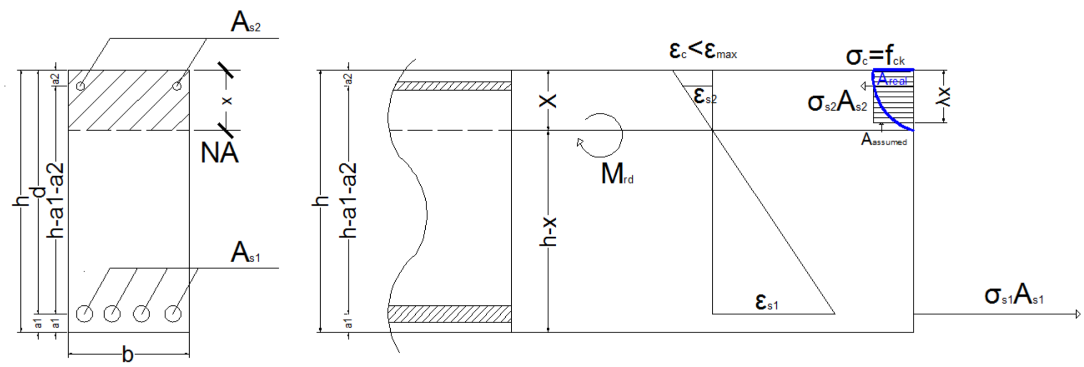

Figure 3.10. Distribution of stresses and strains in the beam.

$$A_{assumed} = 0.8 \cdot A_{real} \tag{3.19}$$

A_{real}	Area of the parabolic distribution
$A_{assumed}$	Area of the rectangle distribution

The stresses in the bottom bars are limited to the yielding stress. Because the top bars are inside the compressed zone it is very unlikely for them to reach yielding stress but nevertheless this has to be checked. According to [Agent, 2008] in order for the top reinforcement to yield, the height of the compressed zone has to be twice the height of the concrete cover so Equation (3.25) has to be checked. The height of the concrete cover considered is 35 mm.

$$x_{pl} > 2 \cdot a_2 \Rightarrow x_{pl} > 70 \tag{3.20}$$

Firstly it is assumed that the top bars also yield so this means that the stresses are also limited to the yielding stress. This gives a new set of initial conditions which are the following:

$$\sigma_{s1} = f_{yk} \tag{3.21}$$
$$\sigma_{s2} = f_{yk} \tag{3.22}$$

f_{yk}	Characteristic strength of steel

Equilibrium of forces is being considered on the horizontal axis which has the Equation (3.23)

$$\sigma_{s1} \cdot A_{s1} - \sigma_{s2} \cdot A_{s2} - \sigma_c \cdot x_{pl} \cdot b = 0 \tag{3.23}$$

By substituting the stresses σ_c, σ_{s1} and σ_{s2} with their limit values, the new equilibrium is Equation (3.24).

$$f_{yk} \cdot A_{s1} - f_{yk} \cdot A_{s2} - f_{ck} \cdot x_{pl} \cdot b = 0 \tag{3.24}$$

From this equation the height of the compressed concrete zone, x_{pl}, is isolated and Equation (3.25) is formed.

$$x_{pl} = \frac{(A_{s2} - A_{s1}) \cdot f_{yk}}{b \cdot f_{ck}} \tag{3.25}$$

The obtained height of the compressed concrete zone is 50.39 mm which doesn't fulfill Equation (3.20), which means that the initial assumption was not correct so the top rebars don't yield. This was expected as it was initially considered that the beam will only be subjected to normal loads and not exceptional loads, for example loads from earthquake.

Because the initial assumption is incorrect, a new distribution of stresses where the top reinforcement doesn't yield is seen in Figure 3.11.

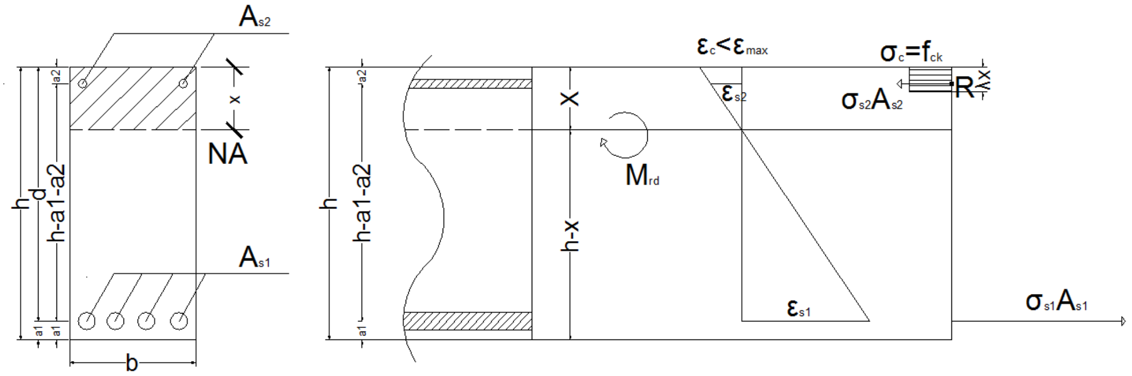

Figure 3.11. Distribution of stresses in the beam.

In this case the height of the compressed zone can't be computed. To calculate the capable moment M_{rd}, equilibrium of bending moments is applied around point R and gives Equation (3.26).

$$\sigma_{s1} \cdot A_{s1} \cdot (d - a_2) + b \cdot x_{pl} \cdot \sigma_c \cdot (a_2 - \frac{x_{pl}}{2}) - M_{rd} = 0$$
$$M_{rd} = \sigma_{s1} \cdot A_{s1} \cdot (d - a_2) + b \cdot x_{pl} \cdot \sigma_c \cdot (a_2 - \frac{x_{pl}}{2}) \tag{3.26}$$

By substituting the stresses in the concrete and in the rebars with the maximum allowed stresses it is obtained Equation (3.27).

$$M_{rd} = f_{yk} \cdot A_{s1} \cdot (d - a_2) + b \cdot x_{pl} \cdot f_{ck} \cdot (a_2 - \frac{x_{pl}}{2}) \tag{3.27}$$

According to Agent [2008], when the compressed zone is small, as seen from the Figure 3.11, it can be ignored from calculating moment capacity so the final formula becomes Equation (3.28).

$$M_{rd} = f_{yk} \cdot A_{s1} \cdot (d - a_2) \tag{3.28}$$

The obtained capable moment M_{rd} is $2 \times 10^8\,\mathrm{N} \times \mathrm{mm}$ which has to be transformed in load bearing capacity and is done with the Equation (3.29).

$$M_{rd} = q_{cap} \cdot \frac{L^2}{8} \tag{3.29}$$

M_{rd}	Moment capacity of the beam
q_{cap}	Load bearing capacity of the beam
L	Length of the beam

From this formula the load bearing capacity is isolated and its value is determined with Equation (3.30).

$$q_{cap} = 8 \cdot \frac{M_{rd}}{L^2} \tag{3.30}$$

The obtained load bearing capacity is 16.03 N/mm.

3.2.4 Displacements

In order to find the maximum displacement of the beam, from Euler-Bernoulli beam theory, Equation (3.31).

$$\delta = \frac{5}{384} \cdot \frac{q_{cap} \cdot l^4}{E \cdot I} \tag{3.31}$$

δ	Displacement
q_{cap}	Load bearing capacity
l	Span of beam
E	Young's Modulus
I	Moment of inertia

Because the section is a composed one, an equivalent bending stiffness has to be calculated. Having the fact that the cross-section is not symmetric on both direction, the centroid of the cross-section is displaced. By having a larger area of the bottom reinforcement bars than the top reinforcement bars, the centroid is displaced toward the bottom reinforcement. In Figure 3.12 the new centroid of the cross-section is seen.

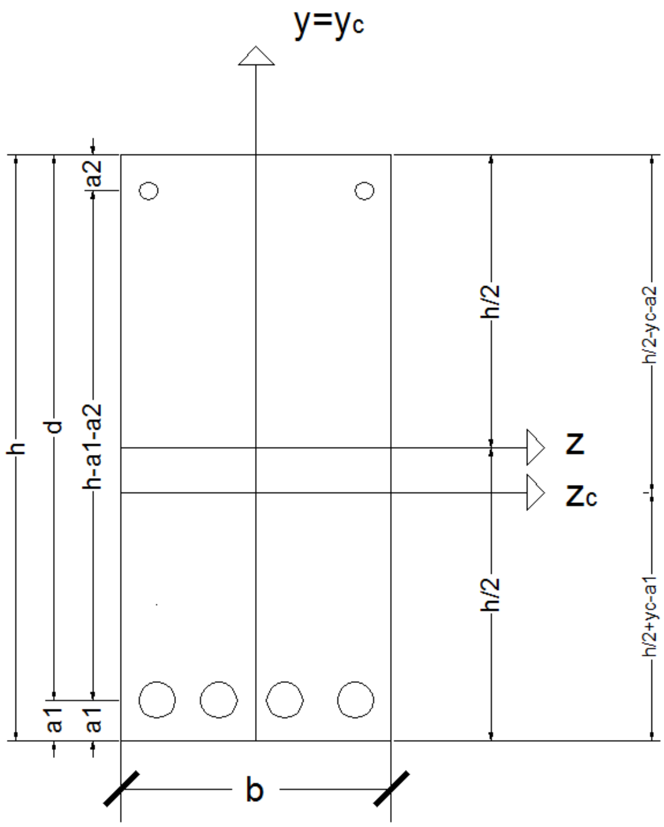

Figure 3.12. Centroid of the cross-section.

In order to find the position of the new centroid an equation is required from where the coordinate of the centroid is isolated. The equation of the static moment is used. The formula to of the static moment is Equation (3.32).

$$S_z = \sum(y_i \cdot A_i) = y_c \cdot A_T \tag{3.32}$$

S_z	Static moment
y_i	Position relative to the centroid
A_i	Area of object relative to the centroid
y_c	Coordinate of the centroid
A_T	Total area of the cross-section

As the cross-section is not homogeneous Young's modulus for different materials has to be taken into account so the new equation of the static moment is Equation (3.33)

$$S_z \cdot E_i = \sum(y_i \cdot A_i \cdot E_i) = y_c \cdot A_T \cdot \sum(\frac{A_i}{A_T} \cdot E_i) \tag{3.33}$$

The equation is expanded for the cross-section as Equation (3.34).

$$
\begin{aligned}
&-(\frac{h}{2}-a_1)\cdot A_{s1}\cdot E_s\cdot 4+(\frac{h}{2}-a_2)\cdot A_{s2}\cdot E_s\cdot 2\\
&-(-(\frac{h}{2}-a_1)\cdot A_{s1}\cdot E_c\cdot 4+(\frac{h}{2}-a_2)\cdot A_{s2}\cdot E_c\cdot 2\\
&=y_c\cdot b\cdot h\cdot(\frac{A_{s1}+A_{s2}}{A_t}\cdot+\frac{A_T-(A_{s1}+A_{s2})}{A_t}\cdot E_c)
\end{aligned}
\tag{3.34}
$$

From this y_c is isolated and can is computed with Equation (3.35)

$$
y_c=\frac{(\frac{h}{2}-a_1)\cdot A_{s1}\cdot(E_c-E_s)+(\frac{h}{2}-a_2)\cdot A_{s2}\cdot(E_s-E_c)}{(A_{s1}+A_{s2})\cdot E_s+(b\cdot h-(A_{s1}+A_{s2}))\cdot E_c}
\tag{3.35}
$$

The position of the new centroid axis is at a distance of $-9.76\,\mathrm{mm}$ from the center of the cross-section. The minus sign shows that, as expected, the centroid is displaced toward the bottom reinforcement. With the new centroid calculated, the equivalent bending stiffness can be computed.

The idea behind the computation of the equivalent bending stiffness is that the concrete is being "removed" from the cross-section and rebars are introduced in the removed holes. The general formula to compute the equivalent bending stiffness is Equation (3.36).

$$
E\cdot I=\sum E_i\cdot y^2\cdot d\cdot A_i
\tag{3.36}
$$

For the current cross-section the formula becomes Equation (3.37)

$$
\begin{aligned}
E\cdot I=&\frac{1}{12}\cdot b\cdot h^3\cdot E_c+b\cdot h\cdot y_c^2\cdot E_c-\\
&-(4\cdot\frac{\pi}{4}\cdot(\frac{\phi_1}{2})^4+4\cdot A_{s1}\cdot(\frac{h}{2}-a_1)^2+2\cdot\frac{\pi}{4}\cdot(\frac{\phi_2}{2})^4+2\cdot A_{s2}\cdot(\frac{h}{2}-a_2)^2)\cdot E_c+\\
&+(4\cdot\frac{\pi}{4}\cdot(\frac{\phi_1}{2})^4+4\cdot A_{s1}\cdot(\frac{h}{2}-a_1)^2+2\cdot\frac{\pi}{4}\cdot(\frac{\phi_2}{2})^4+2\cdot A_{s2}\cdot(\frac{h}{2}-a_2)^2)\cdot E_s
\end{aligned}
\tag{3.37}
$$

By using the common factor of E_c and E_s the previous formula becomes Equation (3.38)

$$
\begin{aligned}
E\cdot I=&\frac{1}{12}\cdot b\cdot h^3\cdot E_c+b\cdot h\cdot y_c^2\cdot E_c+\\
&+(4\cdot\frac{\pi}{4}\cdot(\frac{\phi_1}{2})^4+4\cdot A_{s1}\cdot(\frac{h}{2}-a_1)^2+2\cdot\frac{\pi}{4}\cdot(\frac{\phi_2}{2})^4+2\cdot A_{s2}\cdot(\frac{h}{2}-a_2)^2)\cdot(E_s-E_c)
\end{aligned}
\tag{3.38}
$$

The obtained equivalent bending stiffness is $1.79\times10^{14}\,\mathrm{Nmm}^2$ and is introduced in Equation (3.31). From Equation (3.31) a maximum displacement of $10.79\,\mathrm{mm}$ for the load bearing capacity calculated with the linear-elastic approach and 11.65 mm for the load bearing capacity calculated with the fully plastic approach.

The results for the load bearing capacity and maximum displacements are seen in 3.1.

Table 3.1. Load bearing capacity of different approaches.

Type of beam	Load bearing capacity [N/mm]	Maximum displacement [mm]
Plain concrete	8.45	5.52
Reinforced concrete (Linear-elastic approach)	14.85	10.79
Reinforced concrete (Fully plastic approach)	16.03	11.65

From the Table 3.1 it is seen an increase of 90% in load bearing capacity and an increase of 110% of the maximum allowed deflection. From this it is observed that the rebars have a big influence on the strength of a beam.

Numerical beam design 4

In this chapter a numerical approach is used in order to calculate the bearing capacity and maximum displacements of a 3D concrete beam due to an external load.

The numerical approach is done with the help of Abaqus which is a 3D finite element analysis software. The same beams which were calculated in the previous chapter will now be modeled and the results will be compared with the ones obtained from the analytic analysis.

4.1 Concrete damage plasticity

The main failure mechanism for concrete are crushing under compression and cracking under tension and concrete is known to be a highly plastic material. Abaqus has different ways of modeling plasticity, from simple ones which only take into account, compression and tensile strengths, to more complex one which take into account various phenomena which happen during loading of a concrete element. The concrete damage plasticity is the most complex one. According to [Simulia, 2016] concrete damage plasticity:

- Provides a general capability for modeling concrete and other quasi-brittle materials in all types of structures (beams, trusses, shells, and solids);
- Uses concepts of isotropic damaged elasticity in combination with isotropic tensile and compression plasticity to represent the inelastic behavior of concrete;
- Can be used for plain concrete, even though it is intended primarily for the analysis of reinforced concrete structures;
- Can be used with rebar to model concrete reinforcement; is designed for applications in which concrete is subjected to monotonic, cyclic, and/or dynamic loading under low confining pressures;
- Consists of the combination of nonassociated multi-hardening plasticity and scalar (isotropic) damaged elasticity to describe the irreversible damage that occurs during the fracturing process;

The stress-strain curves are seen in Figure 4.1.

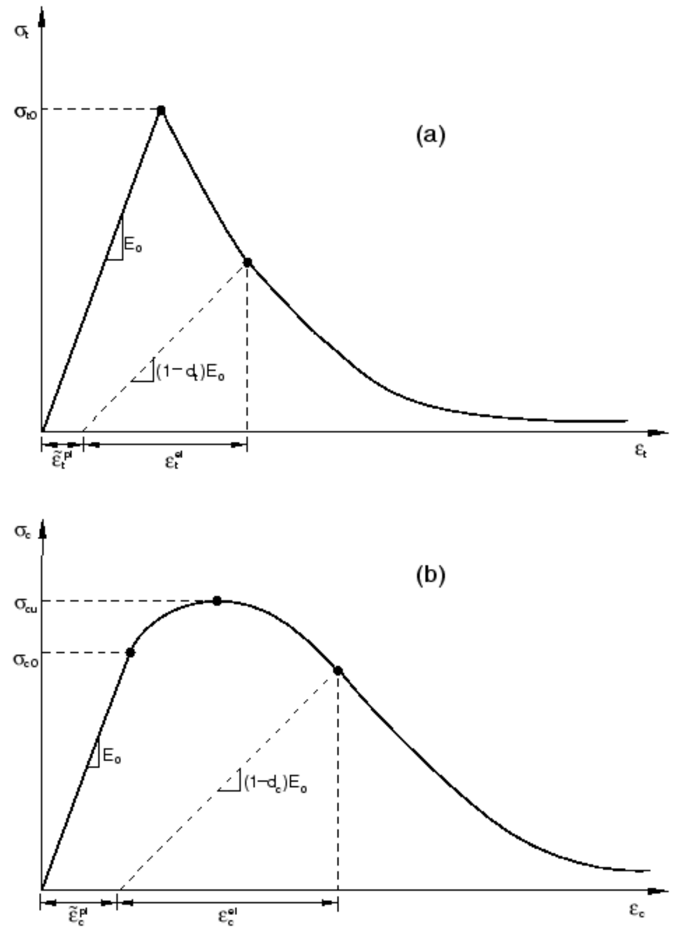

Figure 4.1. Stress-strain curves. Case a)Uniaxial tension. Case b)Uniaxial compression. [Simulia, 2016]

As seen in the figures, at any point after $\sigma_t 0$ or $\sigma_c u$ the unloading doesn't produce a perfect response, this is due to the degradation of the elastic stiffness of the material. The damage of the material is represented by the coefficients d_t and d_c which are function of plastic strain, temperature and field variables. Their value range from zero, which means the concrete is undamaged, up to one, which means total loss of strength. The stress-strain relationships are seen in Equation (4.1).

$$\begin{aligned} \sigma_t &= (1 - d_t) \cdot E_0 \cdot (\varepsilon_t - \tilde{\varepsilon_t}^{pl}) \\ \sigma_c &= (1 - d_c) \cdot E_0 \cdot (\varepsilon_c - \tilde{\varepsilon_c}^{pl}) \end{aligned} \tag{4.1}$$

σ_t	Tensile stress
σ_c	Compression stress
d_t	Damage coefficient for tension
d_c	Damage coefficient for compression
E_0	Initial Young's modulus
ε_t	Tensile strain
ε_c	Compression strain
$\tilde{\varepsilon_t}^{pl}$	Equivalent plastic strain in tenstion
$\tilde{\varepsilon_c}^{pl}$	Equivalent plastic strain in compression

The yielding surface is determined by the effective tensile and compression stresses. The effective stresses are given by Equation (4.2).

$$\begin{aligned} \bar{\sigma_t} &= \frac{\sigma_t}{1-d_t} = E_0 \cdot (\varepsilon_t - \tilde{\varepsilon_t}^{pl}) \\ \bar{\sigma_c} &= \frac{\sigma_c}{1-d_c} = E_0 \cdot (\varepsilon_c - \tilde{\varepsilon_c}^{pl}) \end{aligned} \tag{4.2}$$

$\bar{\sigma_t}$	Effective tensile stress
$\bar{\sigma_c}$	Effective compression stress

According to [Simulia, 2016], the model is based on the yield function of Lublinier et. al (1989), with the additional modifications of Lee and Fenves (1998). The modifications account for the evolution of strength under tension and compression, which affect the evolution of the yield surface by the hardening variables $\tilde{\varepsilon_t}^{pl}$ and $\tilde{\varepsilon_c}^{pl}$. The yielding function is presented in Equation (4.3).

$$\begin{aligned} F &= \frac{1}{1-\alpha} \cdot (\bar{q} - 3 \cdot \alpha \cdot \bar{p} + \beta \cdot (\tilde{\varepsilon}^{pl}) \langle \hat{\bar{\sigma}}_{max} \rangle - \gamma \langle -\hat{\bar{\sigma}}_{max} \rangle) - \bar{\sigma_c} \cdot (\tilde{\varepsilon_c}^{pl}) \\ \alpha &= \frac{(\sigma_{b0}/\sigma_{c0}) - 1}{2 \cdot (\sigma_{b0}/\sigma_{c0}) - 1}; 0 \leq \alpha \leq 0.5 \\ \beta &= \frac{\bar{\sigma_c} \cdot \tilde{\varepsilon_c}^{pl}}{\bar{\sigma_t} \cdot \tilde{\varepsilon_t}^{pl}} \cdot (1-\alpha) - (1+\alpha) \\ \gamma &= \frac{3 \cdot (1-K_c)}{2 \cdot K_c - 1} \end{aligned} \tag{4.3}$$

$\hat{\bar{\sigma}}_{max}$	Maximum principal effective stress
σ_{b0}/σ_{c0}	Ratio of initial equibiaxial compression yield stress to initial uniaxial compression yield stress;
K_c	Ratio of the second stress invariant on the tensile meridian, to that on the compressive meridian, at initial yield for any given value of the pressure invariant p such that the maximum principal stress is negative.
$\bar{\sigma_t} \cdot \tilde{\varepsilon_t}^{pl}$	Effective tensile cohesion stress
$\bar{\sigma_c} \cdot \tilde{\varepsilon_c}^{pl}$	Effective compression cohesion stress

The yield surface in deviatoric plane is seen in Figure 4.2 and the yield surface in plane stress is seen in Figure 4.3.

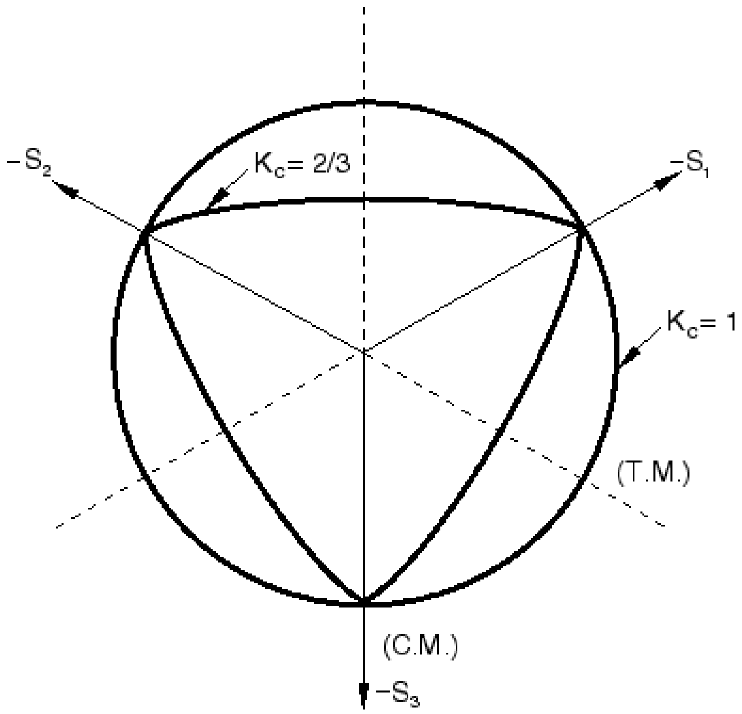

Figure 4.2. Yield surface in deviatoric plane. [Simulia, 2016]

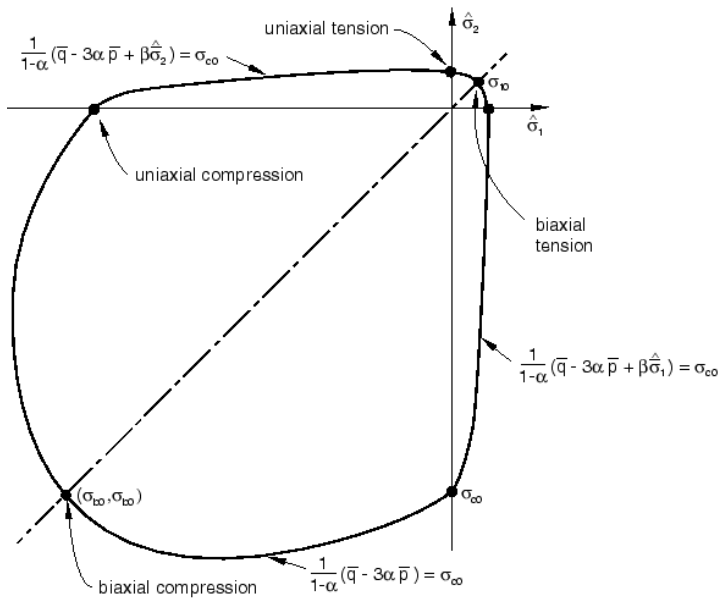

Figure 4.3. Yield surface in plane stress. [Simulia, 2016]

In the report the beams are constituted of concrete and steel reinforcement, subjected to monotonic loading with no confinement so in order to get results close to real life conditions, the concrete is modeled with this type of plasticity.

4.2 Plain Concrete Beam

Firstly in order to verify that the modeling in Abaqus is done correctly, a simple type of beam will be created. The easiest type is a concrete beam which is considered to behave linear elastic with no plasticity. It is well known that concrete is a plastic material so this model is solely done in order to verify that the modeling in Abaqus is done correctly.

4.2.1 Beam model

The beam is modeled as a homogeneous solid having the same cross-section as the analytic beam, with a height of 650 mm and a width of 300 mm. Because this time it is a 3D model a "depth" is also required to be inputted. Typically the depth of the beam should be the length of the beam of 10 000 mm, but because in Abaqus the beam has to be supported in order for the analysis to work an extra 100 mm will be added to the length of the beam. The final length of the beam is 10 100 mm but the distance between the supports will still be 10 000 mm, this way the beam is still the same as the analytic one.

The model is seen in Figure 4.4.

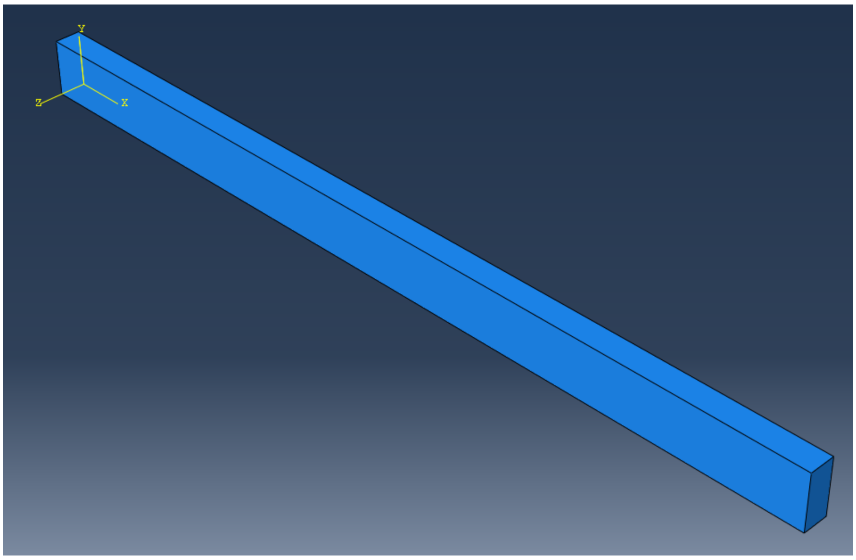

Figure 4.4. 3D model of the beam.

4.2.2 Materials

After the beam is modeled, material properties have to be assigned to it. The beam is a homogeneous beam, which means it is made only of one type of material.

Concrete

Because a linear-elastic analysis is done, Young's modulus and Poison's ratio are defined when a material is created. The Young's modulus used in creating the concrete material is 30 000 $\mathrm{N/mm^2}$ and the Poison's ratio of 0.2, which are the values for C20/25 concrete. Material properties of concrete are presented in Chapter 2.

4.2.3 Analysis

When the model has its material assigned then in order to be able to run the analysis the boundary conditions and loads are defined.

Boundary Conditions

The model has the same static scheme as the analytic beam so it is simply supported. In order to avoid infinite stresses in one point the supports are modeled as metal plates. This is also done to reflect real life testing of a beam. The support plates have the height of the cross-section of 100 mm, the width of 300 mm and thickness of 20 mm. The support plate attached to the beam is seen in Figure 4.5.

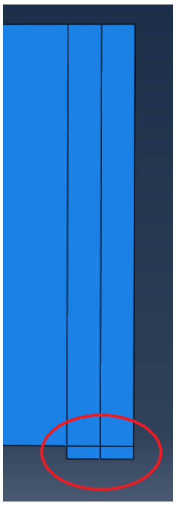

Figure 4.5. Model of the support plate attached to beam.

The boundary conditions are assigned in order to block displacement and rotation on one or more directions, because of this it is imperative that the correct displacements are blocked or else the obtained results will have no meaning. In one of the supports the displacement on Y and Z directions are blocked and in the other support only the Y direction is blocked which is seen in Figure 4.6.

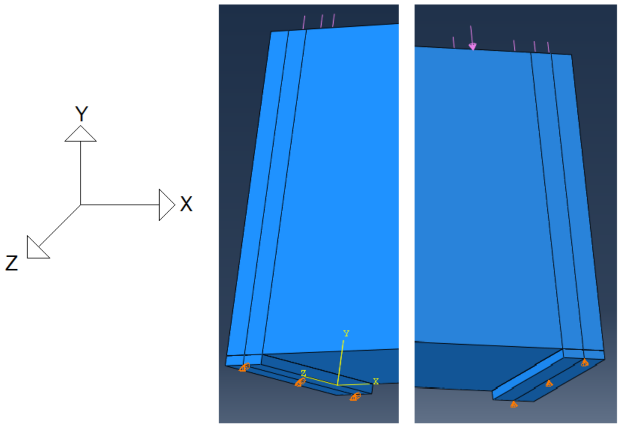

Figure 4.6. The boundary conditions for both supports.

Loading

The load applied on the model has the same magnitude as the load seen in Table 3.1. In order to be able to apply the load from the analytic case, which is a uniformly distributed line load, it has to be transformed in a uniformly distributed surface load. This is done by dividing the magnitude of the load to the width of the model cross-section as seen in Equation (4.4).

$$Q = \frac{q_{cap}}{b} \tag{4.4}$$

Q	Uniformly distributed surface load
q_{cap}	Uniformly distributed line load (Taken for plain concrete beam)
b	Width of model cross-section

The resulting uniformly distributed surface load has a magnitude of $0.028\,\mathrm{N/mm^2}$ and is seen in Figure 4.7. It is applied on the surface between the initial length of beam of 10.000 mm.

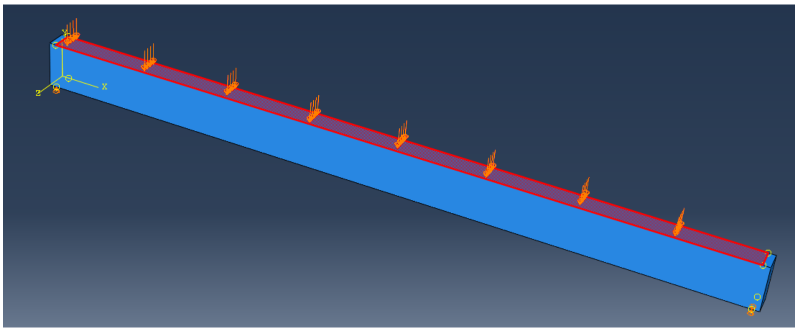

Figure 4.7. The surface of the applied load.

In order to get more accurate results from the analysis the load is applied in increments. In this case the minimum increment is 1×10^{-5} and the maximum increment allowed is 0.1.

If the model doesn't fail it means that its load bearing capacity is higher than the applied surface load so a higher load than the previous one will be applied in order to produce failure.

Meshing

The model has to be segmented in multiple finite elements in order to see the way the model behaves. To do this the model is meshed. Abaqus has various type of elements which can be used for meshing, for example:

- Tetrahedral
- Hex

The mesh formed by tetrahedral elements are best used when dealing with complicated geometry, for example circular cuts, as the mesh is more fine around key spots of the model. The tetrahedral elements can be 4-node or 10-node. The 10-node element will give more accurate results as they have a higher number of degrees of freedom but at the same the time the computational power needed to run the model is also higher. A sketch of the tetrahedral elements is seen in Figure 4.8 and a model meshed with tetrahedral elements can be seen in Figure 4.9.

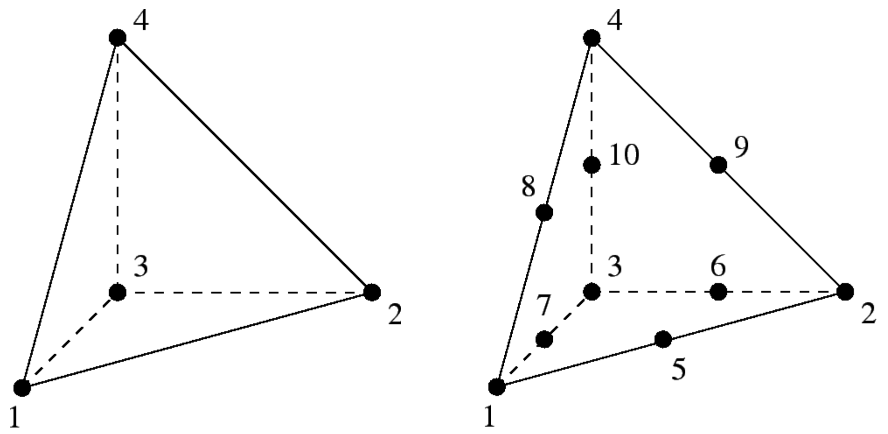

Figure 4.8. Sketch of the tetrahedral elements. [MIT, 2014]

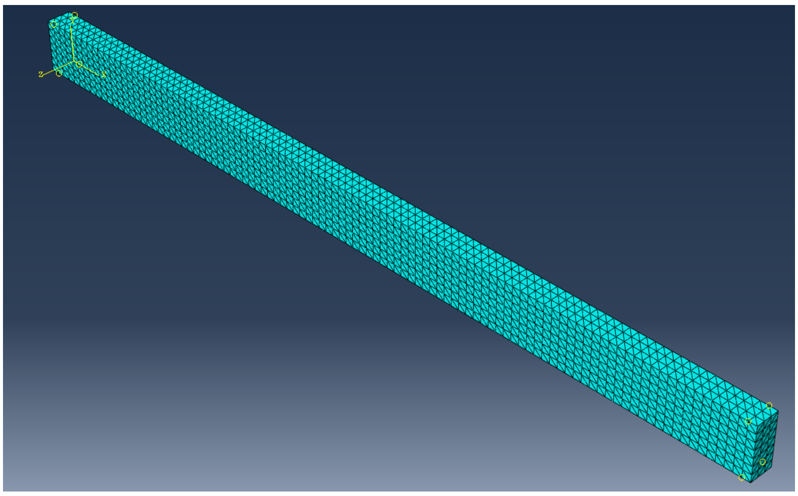

Figure 4.9. The beam meshed with tetrahedral elements.

The mesh formed by hex elements are better for simple geometry model. While this type of meshing provides less accurate results, but with no important difference, the computational time is far less then tetrahedral elements as the mesh will consist of smaller number of elements. The hex elements can be 8-node or 20-node, as with the previous case the 20-node element mesh having more accurate results than the 8-node but requiring a larger amount of computational power. A sketch of the tetrahedral elements is seen in Figure 4.10 and a model meshed with tetrahedral elements is seen in Figure 4.11.

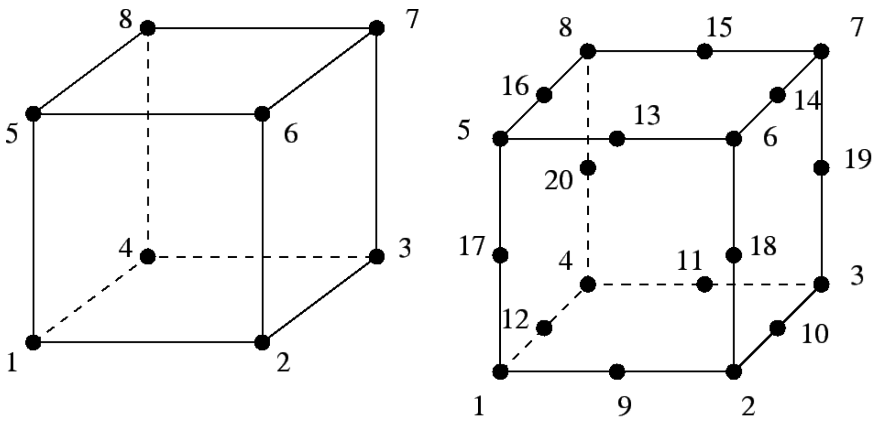

Figure 4.10. Sketch of the hex elements. [MIT, 2014]

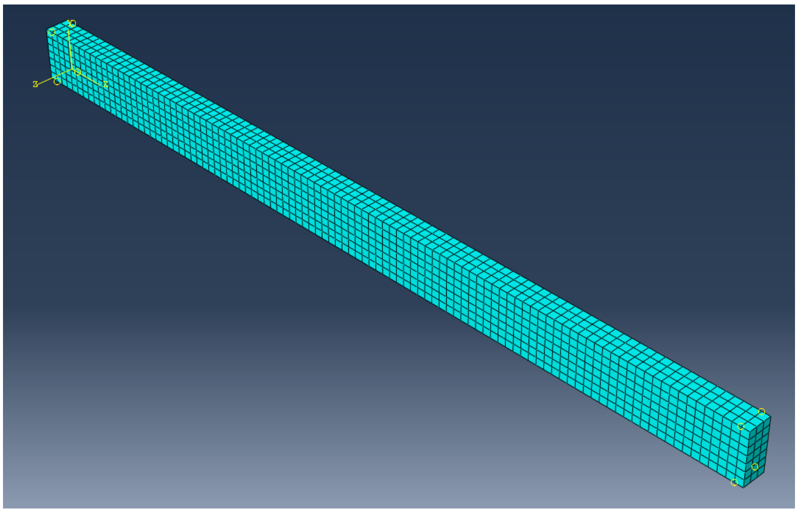

Figure 4.11. The beam meshed with hex elements.

Because this model is a simple one with no complicated geometries or complicated cross-section, four analysis with different types of elements has been done in order to compare the difference in displacements and time required to run the analysis.

Table 4.1. Displacement and time for different meshes.

Type of element	Degrees of freedom	Displacement [mm]	Time [s]
4-node tetrahedral	180 840	5.067	35
10-node tetrahedral	452 100	5.337	45
8-node hex	50 904	5.459	26
20-node hex	127 260	5.337	33

Because the 8-node hex elements mesh has the quickest analysis time and also the closest result to the analytic calculation, for the next models the mesh will consist of this type of element.

Convergence analysis

Different type of meshes produce various results so a balance between accuracy and computational power is required and in order to do this a convergence analysis is performed. This is done by making the mesh finer or coarser. The finer the mesh is the more accurate are the results but more computational power is required. The maximum displacement is calculated for the same uniformly distributed load and is compared for different types of meshes. The results are seen in Table 4.2 and presented as graph in Figure 4.12.

Table 4.2. Maximum displacements for different meshes.

Mesh size mm	Number of degrees of freedom	Maximum displacement [mm]	Time [s]
25	3 025 152	5.356	287
50	378 144	5.380	40
75	115 776	5.418	22
100	50 904	5.459	14
125	19 440	5.566	12
150	13 056	5.697	12
175	11 328	5.692	11
200	7488	5.999	11

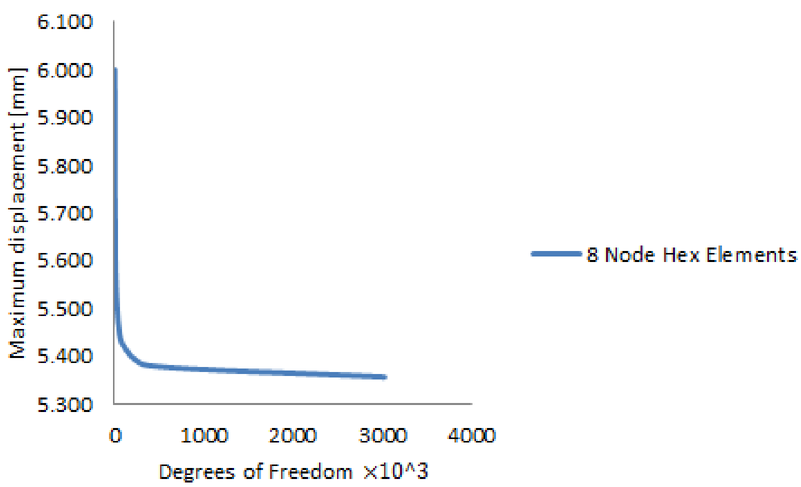

Figure 4.12. Maximum displacement for different meshes.

From the results it is seen that the maximum displacement which is closest to the analytic result is obtained when the mesh size is 100 mm. This is the best balance between result accuracy and computational time. The next models will have a mesh size of 100 mm.

Symmetry

In order to reduce the computation time, a symmetry plane is used around the center of the beam. This way the beam is divided into two identical models with half the initial span. The new span of the beam is calculated with Equation (4.5).

$$l = \frac{L}{2} \tag{4.5}$$

l	Half span of the beam
L	Initial span

The new span of the beam is 5 m. Because only half of the beam is considered, the beam becomes statically undetermined so a new support is introduced where the "cut" has been made, which permits rotation but not translation on X direction. The new model of the beam is seen in Figure 4.13.

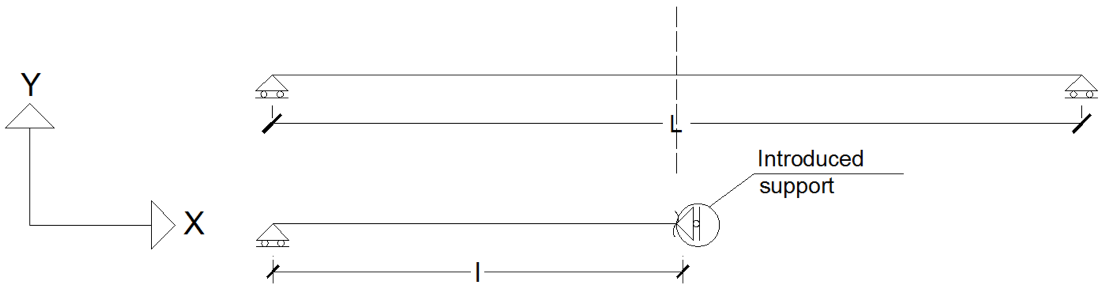

Figure 4.13. The new static scheme of the beam.

4.2.4 Results

With the model now meshed the analysis can be done. After the analysis finished a deformed model is produced seen in Figure 4.14.

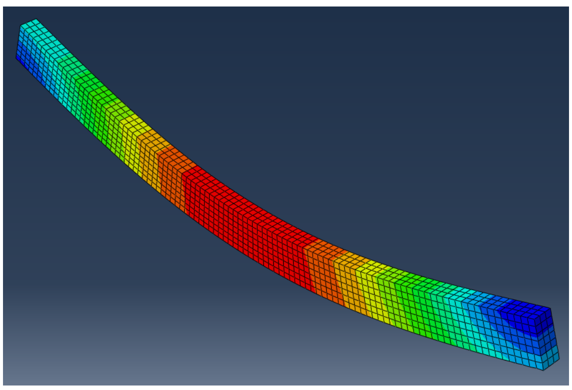

Figure 4.14. Output result of the analysis.

Bearing capacity

The analysis is being run with a model defined by an elastic material so a bearing capacity can not be obtained from Abaqus as the model will never fail and can have infinite displacements.

Displacements

The relevant results are the displacements on Y axis which can are compared with the ones obtained from the analytic analysis. The results should be very close as there will always be differences in accuracy of results between numerical and analytic analysis. This is because a 3D model adds a third dimension to the model and is a more realistic, but can also be because of errors in modeling. The obtained displacement on Y-direction is 5.459 mm and as expected, in concordance with Euler-Bernoulli beam theory, is at the middle of the beam. The results is seen in the table in Figure 4.15

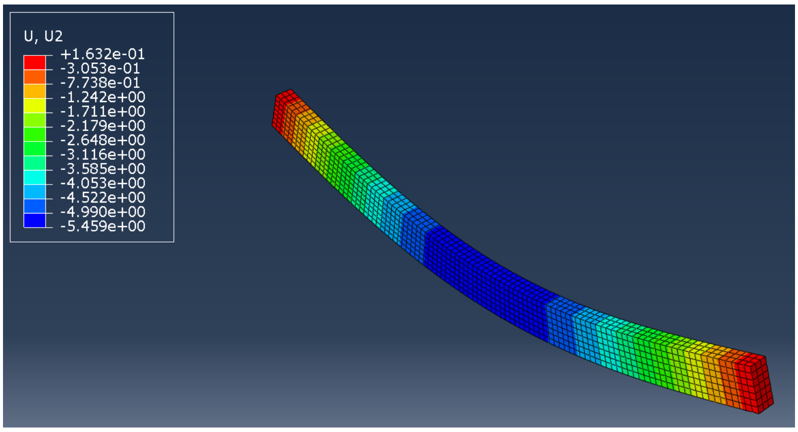

Figure 4.15. Displacement results.

In Table 4.3 is presented the difference between analytic and numerical results. The results are very close so this means that the beam has been modeled correctly and now more complex behavior can be analyzed.

Table 4.3. Displacement results for analytic and numerical analysis.

Type of analysis	Analytic	Numerical	Difference in Percentage
Displacement[mm]	5.52	5.459	1 %

4.2.5 Plasticity

Concrete in real life is a plastic material so in order to see how the beam would behave more realistic plasticity is added to the material properties of the model. A new property named "concrete damaged plasticity" is added.

The plasticity properties are the default ones offered by Abaqus. The compression strength is 20 N/mm^2 and the tensile strength is 1.5 N/mm^2, these are the strength for concrete class C20/25. The behavior of concrete is shown in Chapter 2.

Analysis

All the elements of the analysis, including the boundary conditions, meshing and loading are the same as the previous model.

Results

The analysis is performed identically as before. Because the material is defined as plastic now it means that it can fail under loading so the bearing capacity can now be obtained from the model.

As stated previously the beam is again loaded in increments with load having a magnitude of 0.028 N/mm^2. This time the analysis doesn't finish and this means that at an increment of the load the beam model has failed.

This also is be observed from the obtained Load-Displacement curve as seen in Figure 4.17. The Load-Displacement curve is obtained by choosing a node from the output results, because the maximum displacement is at the middle of the beam, the node chosen will also be at the middle of the beam as seen in Figure 4.16.

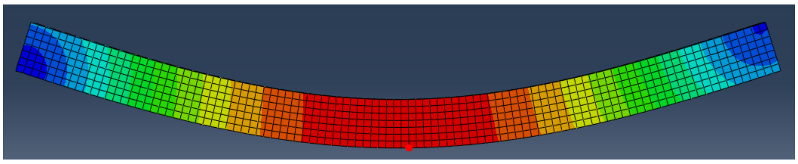

Figure 4.16. Position of the analyzed point.

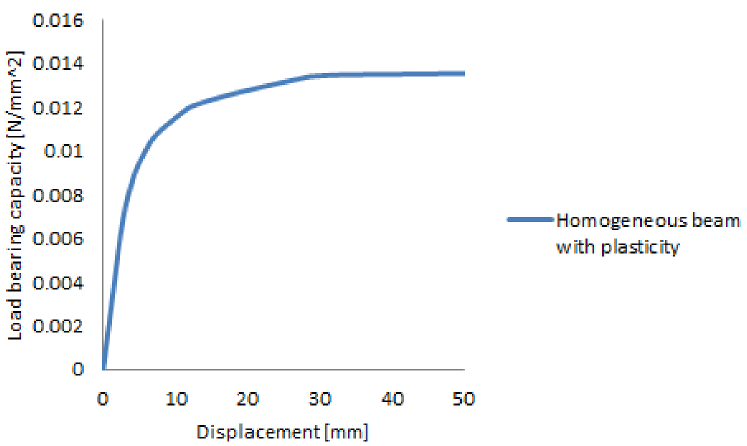

Figure 4.17. Load displacement curve for the load of 0.028 N/mm^2.

The Load-Displacement curve shows that when the beam started to behave plastic it soon failed. This is because concrete behaves poorly in tension. From this the bearing capacity of the model can be computed, this is done with Equation (4.6).

$$Q_{cap} = q_{load} \cdot i_t \tag{4.6}$$

Q_{cap}	Bearing capacity of the beam
q_{load}	Applied load
i_t	Increment

The obtained bearing capacity is 0.014 14 N/mm^2. A new analysis is performed with the model being loaded with the obtained bearing capacity. This is done in order to see if the analysis finishes and acts as a check to see if the results are correct. The analysis finishes this time which means that the model doesn't fail.

The final results of the analysis of the concrete homogeneous beam model are presented in Table 4.4.

Table 4.4. Load bearing capacity.

Type of Analysis	Load Bearing Capacity (Surface) [N/mm^2]	Load Bearing Capacity (Line) [N/mm]
Elastic	0.028 16	8.45
Plastic	0.014 14	4.242

4.3 Reinforced concrete beam

One way of increasing the bearing capacity of the beam is by adding reinforcement to the cross-section.

4.3.1 Beam model

The beam model will no longer be homogeneous as now rebars will be inserted in the cross-section. The concrete part of the beam will be modeled the same as before. For the reinforcement, the rebars can be modeled in two ways:

- Solid element
- Wire element

Both types of models will have the length of 10 100 mm, matching the length of the beam.

The solid rebar is created by the same procedure as the beam. This is seen in Figure 4.18. As mentioned in the analytic analysis, there are two types of rebars used. There are four ϕ20 bars at the bottom and two ϕ10 bars at the top.

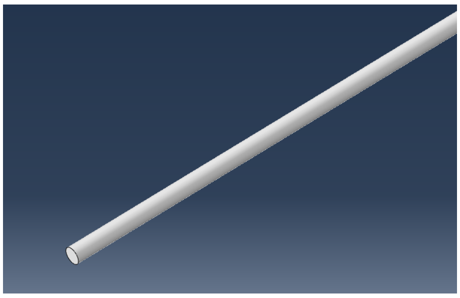

Figure 4.18. Solid rebar model.

The wire rebar is modeled as a wire element and it is assigned to it a circular profile. This is seen in Figure 4.19

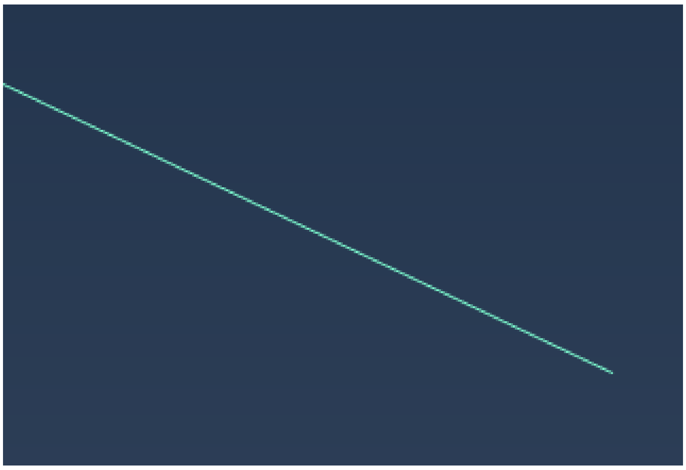

Figure 4.19. Wire rebar model.

The solid rebar model is closer to a real life rebar so the results should be more accurate than that of a wire rebar model. In order to see the difference in the accuracy of the results and computational time between the two types of rebars, two separate beam models have been created each using a different model of the rebar. For the beam and rebars to work together as a whole, conditions have to inputted. For the solid rebars model the beam and the rebars are merged together as a whole piece which resembles more real life conditions and for the wire rebars a constraints has to be assigned between the beam and the rebars. This way Abaqus will embed the rebars inside the beam which will make them work together. The cross-section for the reinforced concrete beam with solid rebars is seen in Figure 4.20. The cross-section of the reinforced concrete beam with wire elements is not shown as the rebars do not appear on the face of the cross-section.

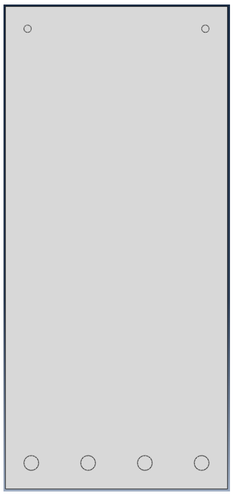

Figure 4.20. Cross-section of reinforced concrete beam with solid rebars.

4.3.2 Materials

The reinforced concrete beam is composed of two type of materials, concrete for the beam cross-section and steel for the rebars.

Concrete

Concrete is defined exactly the same as in the concrete homogeneous model.

Steel

Steel is a ductile material which works very well in tension, this being the reason for its use as reinforcement. For the elastic part, Young's Modulus of $2.1 \times 10^5\,\mathrm{N/mm^2}$ and Poison's ratio of 0.3 are defined and for the plastic part the yielding strength of $275\,\mathrm{N/mm^2}$ is defined.

4.3.3 Analysis

The overall analysis is identical with the one performed for the homogeneous beam.

Boundary Conditions

Same boundary conditions of simply supported beam, which restrict displacements on X and Y directions, are applied as seen in Figure 4.6.

Loading

The loading will be applied on the same surface seen in Figure 4.7. The load applied will be the analytic bearing capacity, calculated in the previous chapter, transformed in a uniformly distributed surface load. The load applied to the beam is $0.053\,\mathrm{N/mm^2}$.

Meshing

For the concrete cross-section 8-node hex elements will be used as stated in the previous analysis in order to save computational power. The meshing will be different for the solid rebars model and for the wire rebar model. For the model with solid rebars it is necessary to create cutting planes in order to make a fine mesh. Firstly cutting planes are created through the middle of each rebar, secondly a cutting plane is created around the Y-axis splitting the beam in two halves seen in Figure 4.21. Lastly three more cutting planes are done around the X-axis each of them splitting the model in smaller half sections as seen in Figure 4.22.

The meshing will be different for the solid rebars model and for the wire rebar model. For the model with solid rebars it is necessary to create cutting planes in order to make a fine mesh. Firstly cutting planes are created through the middle of each rebar, secondly three cutting plane are created around the Y-axis and two around Z-axis splitting the beam in smaller half section as seen in Figure 4.21. Lastly three more cutting planes are done around the X-axis each of them splitting the model in smaller half sections as seen in Figure 4.22. This will let Abaqus choose the appropriate geometry of the elements for each part of the mesh. As is seen in Figure 4.23, the geometries of the hex-elements near the rebar are different than those in other parts of the beam.

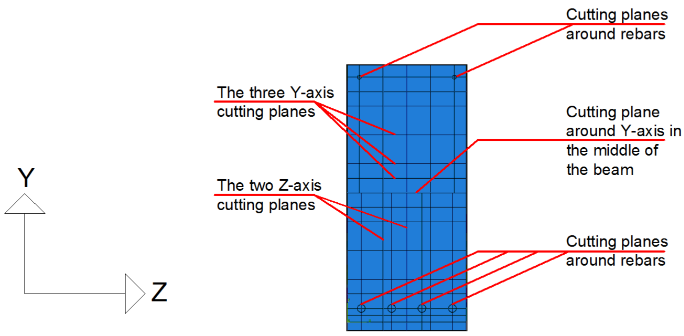

Figure 4.21. Cutting planes around Y-axis, Z-Axis and through the center of the rebars.

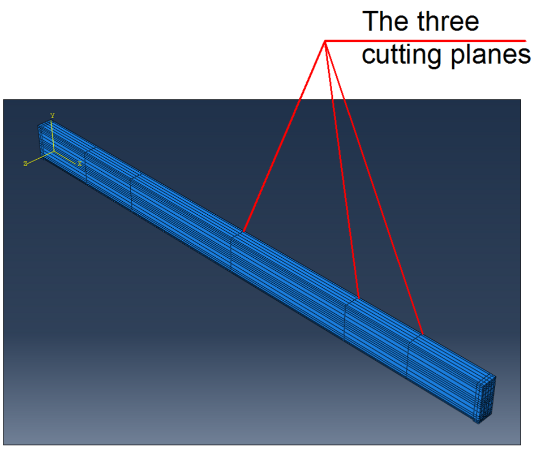

Figure 4.22. Cutting planes around X-axis and through the center of the rebars.

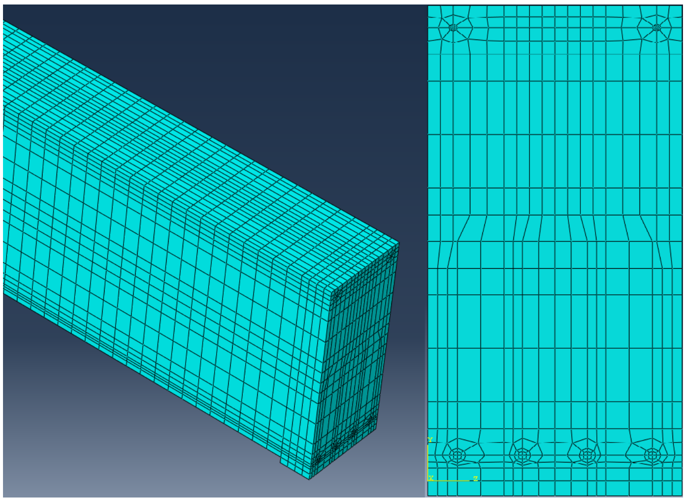

Figure 4.23. Final mesh of the model with solid rebars.

For the wire rebars there is no specific type of meshing. The beam model with wire rebars is meshed the same way as the homogeneous beam.

4.3.4 Results

The results obtained from the analysis are the load bearing capacity and the maximum displacements which are then compared with the analytic results. As mentioned earlier, the time necessary to run the two types of model is also analyzed. The results for the displacements and computational times are seen in Table 4.5.

Table 4.5. Displacement and time for different meshes.

Model type	Solid rebar beam model	Wire rebar beam model	Difference %	Analytic model
Degrees of freedom	2189952	407808	81	[-]
Uniformly distributed Surface load [N/mm^2]	0.053	0.053	[-]	0.053
Maximum displacement [mm]	21.82	20.16	6	11.65
Computational time [s]	1454	141	90	[-]

From the table it is seen that the difference between the obtained displacements from the two numerical models is 7%, but the time required to analyze the wire rebar model is 90% faster than the solid rebar model. Even though the solid rebar beam model is more close to a real life beam, the computational time saved with the wire rebar model is significant, thus the next analyzes will be done on models with wire rebars. It is observed that there is an important difference between the displacements obtained in the analytic and numerical analyses. This is because in the analytic analysis the cross-section is considered with 0 tensile strength, while Abaqus takes into account the tensile strength. The bearing capacity is also analyzed as in the homogeneous beam and compared with the analytic results. As before the beam is loaded with a force greater than the bearing capacity of the analytic model. The load imposed is 0.1 N/mm^2. The wire rebar beam model fails at the increment of 0.747 s, from this it results that the bearing capacity of the beam is 0.0747 N/mm^2. This is an increase of 29% in comparison with the analytic calculation.

4.4 Influence of stirrups

After the analysis of the beam is performed stirrups are added as additional reinforcement. While the rebars support the bending moment acting on the beam, the stirrups are used to support the shear forces. They are disposed transversal on the cross-section. The new cross-section is seen in Figure 4.24.

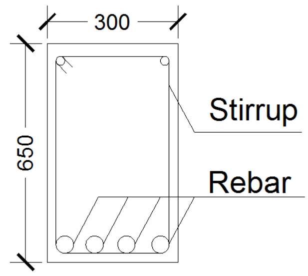

Figure 4.24. Beam cross-section with stirrup.

The distribution of the shear force acting on the beam is seen from Figure 4.25. From this figure it is seen that the highest values of the shear force is at the supports so because of this the distance between the stirrups in the zone near the supports will be 125 mm and the distance between them in the field will be the maximum allowable distance mentioned by [EN 1992-1-1, 2014] which is 250 mm.

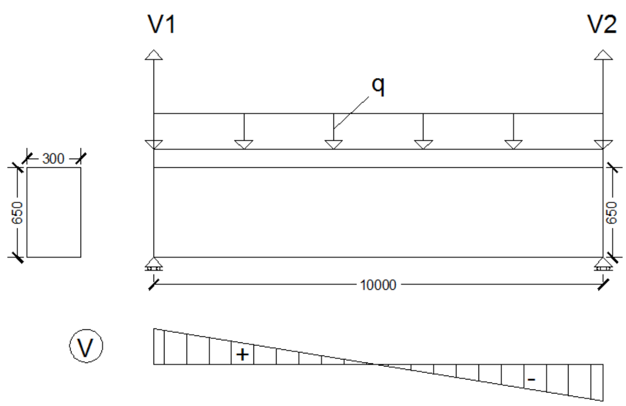

Figure 4.25. Shear force diagram.

4.4.1 Modeling

The stirrups are modeled as wire elements, as demonstrated previously that the difference in results between solid and wire elements are small. The material of which the stirrups are made is S275 steel, the same as the rebars. The diameter of the bars from which the stirrups are manufactured is $\phi 8$. In reality the stirrups are longer than the length required to envelope the rebars, this is done in order to have a region with which the stirrup is tied with the rebars in order to limit its movement. In Abaqus this extra length is not present as it is not necessary, the way the stirrups are made to work together with the cross-section is through assigned constraints. The 10 m beam section is seen in Figure 4.26.

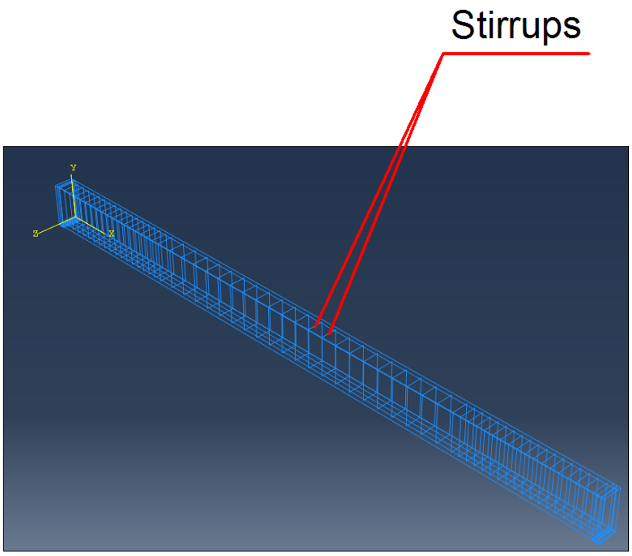

Figure 4.26. Cross-section of the 10 m beam.

4.4.2 Analysis

In order to see how the stirrups influence the bearing capacity, six different reinforced concrete beam models with various lengths are created and the results obtained from their analysis compared. Only the length is modified in the models, all other characteristics remain the same.

4.4.3 Results

The load displacement curve for each model is presented in the following figures.

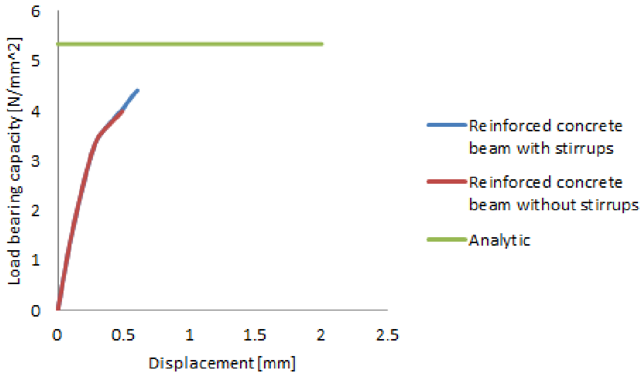

Figure 4.27. Load displacement curve for the 1 m beam.

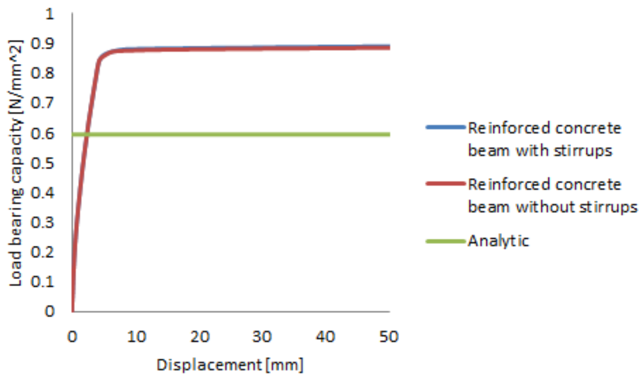

Figure 4.28. Load displacement curve for the 3 m beam.

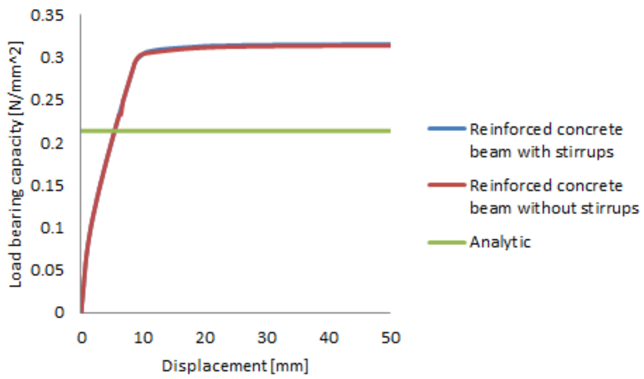

Figure 4.29. Load displacement curve for the 5 m beam.

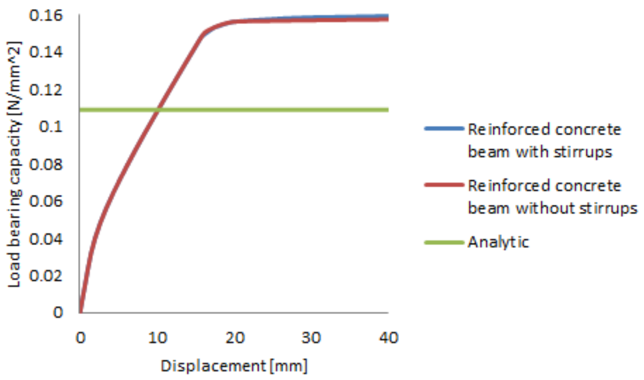

Figure 4.30. Load displacement curve for the 7 m beam.

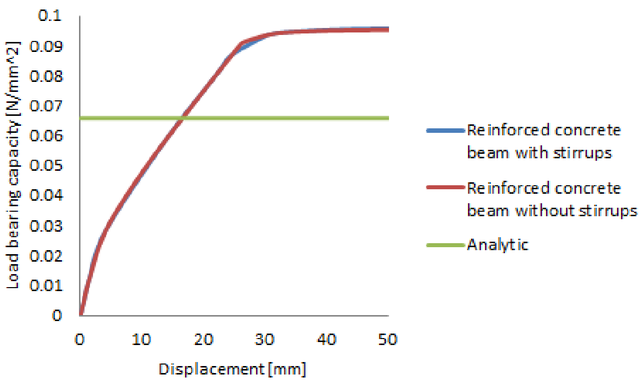

Figure 4.31. Load displacement curve for the 9 m beam.

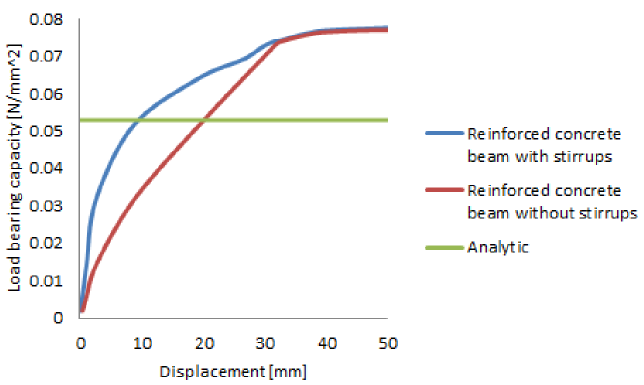

Figure 4.32. Load displacement curve for the 10 m beam.

Table 4.6. Load bearing capacity for the models.

Model type	1 meter beam	3 meter beam	5 meter beam	7 meter beam	9 meter beam	10 meter beam
Bearing capacity without stirrups (Analytic) [N/mm^2]	5.3449	0.5939	0.2138	0.1091	0.0660	0.053
Bearing capacity without stirrups (Numerical) [N/mm^2]	3.995	0.854	0.301	0.154	0.095	0.0747
Bearing capacity with stirrups (Numerical) [N/mm^2]	4.412	0.862	0.308	0.158	0.099	0.0787
Difference in bearing capacity[%]	10	3	3	2	2	2

From this table it is observed that the shorter the beam is the higher the bearing capacity it has. The stirrups don't have a significant influence on the bearing capacity but it is observer that their influence increases as the length of the beam decreases. This happens because the effect of shear forces increase as the length of the beam decreases. The reason why the for the 1 m beam the analytic value is higher than the numerical values, is because in the analytic solution it is assumed to fail due to the effect of the bending moment, but in the numerical model it fails due to shearing.

4.5 Bent reinforcement rebar

According to [EN 1992-1-1, 2014] bent rebars can be used as reinforcement to provide higher bearing capacity in beams. The two top ϕ 10 straight rebars have been replaced with two ϕ 10 bent rebars. They are modeled as wire elements and the model is seen in Figure 4.33. The angle of the bending is 45 deg.

Figure 4.33. Model of the bent rebar.

4.5.1 Analysis

Five models have been created in order to see the influence of bent rebars. The models have the length of 3000 mm, 5000 mm, 7000 mm, 9000 mm, 10 000 mm respectively and their results are compared with the beams of the same length from the previous analysis.

4.5.2 Results

The load displacement curves obtained from the analysis are compared with the ones obtained from the previous models and are seen in Figure 4.34, Figure 4.35, Figure 4.36, Figure 4.37, Figure 4.38.

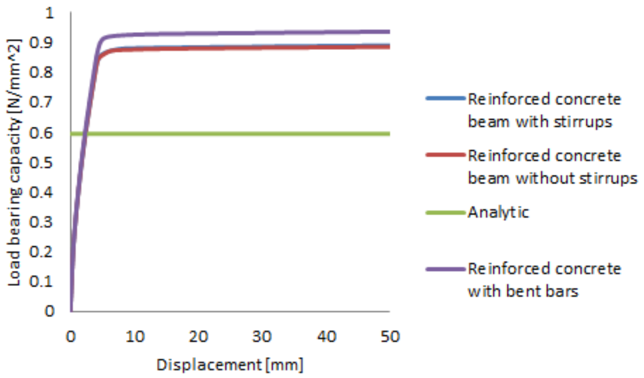

Figure 4.34. Load displacement curve for the 3 m beam.

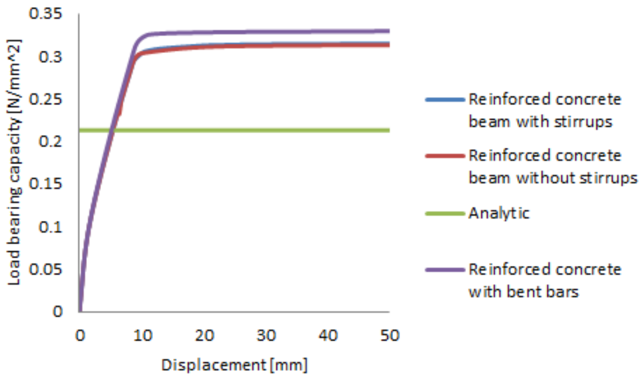

Figure 4.35. Load displacement curve for the 5 m beam.

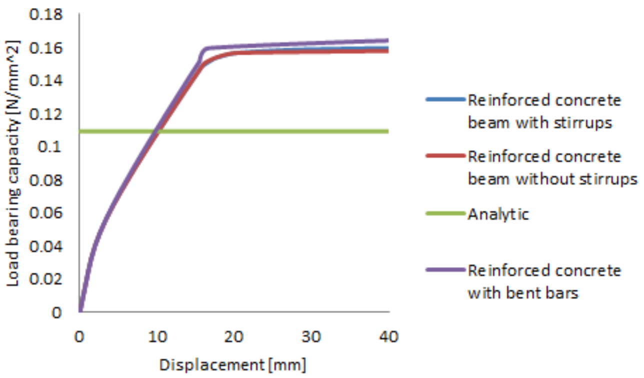

Figure 4.36. Load displacement curve for the 7 m beam.

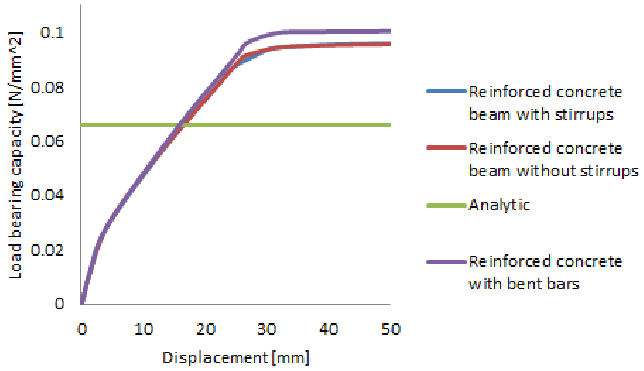

Figure 4.37. Load displacement curve for the 9 m beam.

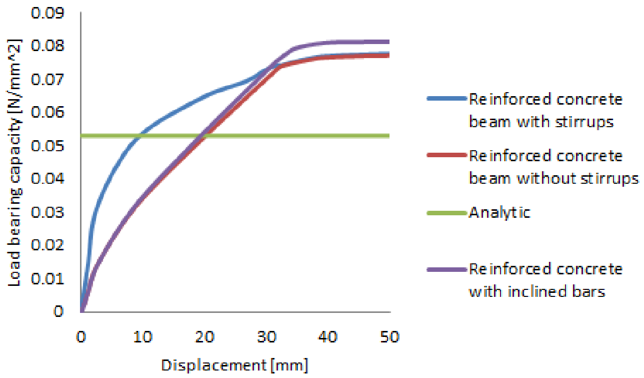

Figure 4.38. Load displacement curve for the 10 m beam.

The results are presented in Table 4.7

Table 4.7. Load bearing capacity for the models.

Model type	3 meter beam	5 meter beam	7 meter beam	9 meter beam	10 meter beam
Bearing capacity without stirrups (Analytic) [N/mm^2]	0.5939	0.2138	0.1091	0.0660	0.053
Bearing capacity without stirrups (Numerical) [N/mm^2]	0.854	0.301	0.154	0.095	0.0747
Bearing capacity with stirrups (Numerical) [N/mm^2]	0.862	0.308	0.158	0.099	0.0787
Bearing capacity with bent rebars (Numerical) [N/mm^2]	0.921	0.326	0.165	0.102	0.0796
Difference in bearing capacity[%]	7.2	8.5	6.8	7	6

From the table it is observed that the bent rebars increase the bearing capacity between 6% and 8.5%, which is more than twice than the increase of 3% obtained by using stirrups. This might be because the bent rebars have a higher reinforcement area than straight rebars.

Analytic Column design 5

In this chapter an analytic approach is used in order to calculate the critical buckling load of a concrete column due to an external load.

The analysis is performed based on calculation from the [EN 1992-1-1, 2014]. A plain concrete column and a reinforced concrete column are compared in terms of critical buckling load.

5.1 Plain concrete column

5.1.1 Column model

As in the case of the beam, the column is created to resemble as much as possible a real column inside a structure. This is done in order to get more accurate results. The cross-section has a width of 300 mm, a height of 300 mm and a length of 10 000 mm. This is seen in Figure 5.1. The supports of the column are fixed at the bottom and simply supported at the top.

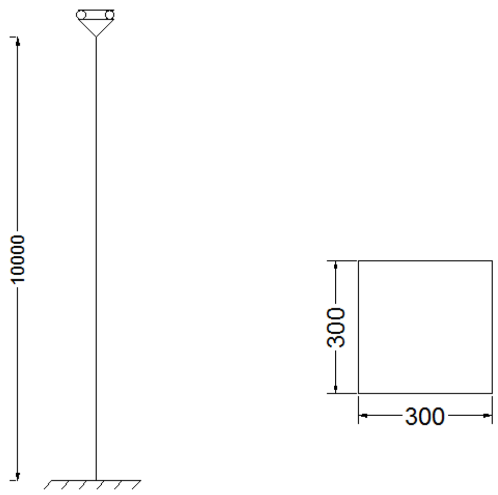

ol

Figure 5.1. Static system and cross-section of the column.

5.1.2 Materials

The column is made of C20/25 concrete with a Young's modulus of 30 000 N/mm^2. The concrete is assumed to act linear-elastic in order to simplify the analysis. This type of behavior is seen in Chapter 2.

5.1.3 Load bearing capacity

A centrally loaded column will compress under loading and at the critical buckling load it will fail by buckling. For a linear-elastic material, as it is currently assumed for the concrete, the critical buckling load is calculated with Euler formula seen in Equation (5.1).

$$N_{cr} = \frac{\pi^2 \cdot E \cdot I}{l_0^2} \tag{5.1}$$

N_{cr}	Critical buckling load
E	Young's modulus of concrete
I	Moment of inertia of the cross-section
l_0	Buckling length

The moment of inertia is calculated with Equation (5.2).

$$I = \frac{b \cdot h^3}{12} \tag{5.2}$$

I	Moment of inertia
b	Width of cross-section
h	Height of cross-section

The buckling length depends on the supports type of the column. According to [Agent, 2008], the calculation for different buckling lengths is seen in Figure 5.2.

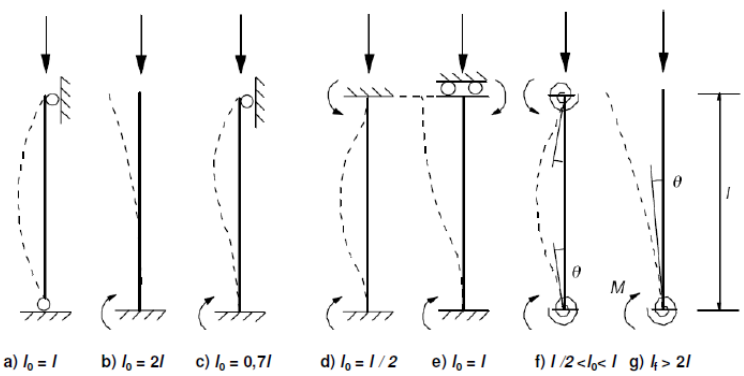

Figure 5.2. Buckling lengths and deformed shapes for different types of supports. [Agent, 2008]

The column will have the buckling length according to case "e" from the Figure 5.2, so the buckling length is 10 000 mm. The critical buckling load obtained is 1.932×10^6 N.

When the concrete is considered to act non-linear, as in real life, the critical buckling stress is computed with Equation (5.3).

$$\sigma_{cr} = \frac{f_{ck}}{1 + \frac{f_{ck}}{\pi^2 \cdot E_{c0k}} \cdot (\frac{l_0}{i})^2} \tag{5.3}$$

σ_{cr}	Critical buckling load
f_{ck}	Compressive strength of concrete
E_{c0k}	Young's modulus of undeformed concrete
l_0	Buckling length
i	Radius of gyration

The radius of gyration is calculated with Equation (5.4).

$$i = \sqrt{\frac{I}{A}} = \sqrt{\frac{\frac{b \cdot h^3}{12}}{b \cdot h}} \tag{5.4}$$

i	Radius of gyration
I	Moment of inertia of the cross-section
A	Area of the cross-section
b	Width of cross-section
h	Height of cross-section

The obtained critical buckling load is obtained by multiplying the critical buckling stress with the area of the concrete cross-section. The value of the critical buckling load is 0.931×10^6 N.

5.2 Reinforced concrete column

The column is now strengthened with the help of reinforcement in order to increase the load bearing capacity. For this type of column it is considered that the materials behave non-linearly.

5.2.1 Column model

The column has the same dimensions and properties as before and now four ϕ 20 rebars are introduced as reinforcements, as seen in Figure 5.3.

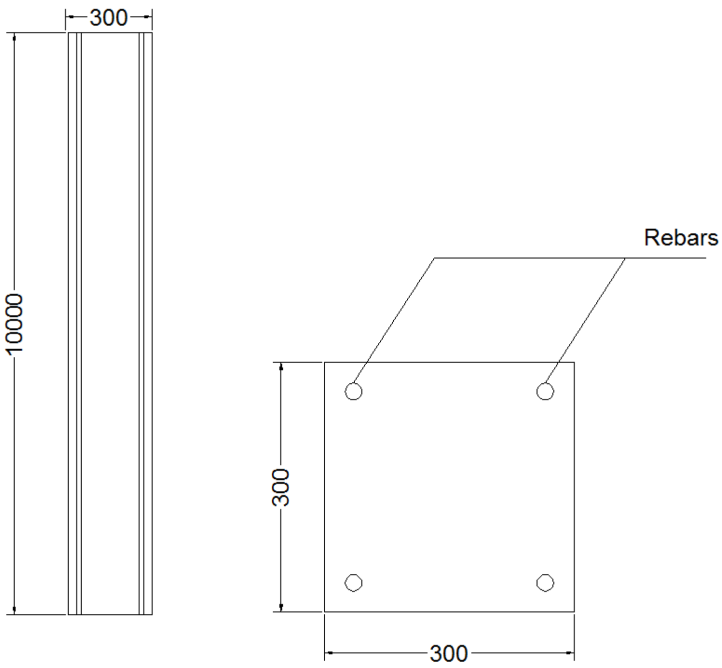

Figure 5.3. Cross-section of reinforced concrete column.

5.2.2 Materials

Along the concrete, S275 steel rebars with a yielding strength of 275 N/mm^2 are added. Behavior of steel is seen in Chapter 2.

5.2.3 Load bearing capacity

The formula to compute the critical buckling load is Equation (5.5).

$$N_{cr} = \sigma_{cr} \cdot (A_c - A_s t) + sigma_{crs} \cdot A_s t \tag{5.5}$$

N_{cr}	Critical buckling load
σ_{cr}	Critical buckling stress of concrete
σ_s	Stress of steel
A_c	Concrete cross-section area
$A_s t$	Reinforcement area

To calculate the stress in steel Equation (5.6) is used.

$$\sigma_s = \frac{\sigma_{cr} \cdot E_c}{E_s} \tag{5.6}$$

σ_s	Stress in steel
σ_{cr}	Critical buckling stress of concrete
E_c	Young's modulus of concrete
E_s	Young's modulus of steel

The area of steel is the area of the four ϕ 20 rebars. The area of concrete is the area of the concrete cross-section. The critical buckling load is 1.013×10^6 N

The critical buckling loads obtained are seen in Table 5.1.

Table 5.1. Load bearing capacity of different approaches.

Type of column	Critical buckling load [$\mathrm{N} \cdot 10^6$]
Plain concrete (Linear-elastic)	1.932
Plain concrete (Non-linear)	0.931
Reinforced concrete (Non-linear)	1.013

From the previous table is observed that the reinforcement increase the critical buckling load by 8%.

Numerical column design 6

In this chapter a numerical approach is used in order to calculate the bearing capacity of a 3D concrete column.

The numerical approach is done with the help of Abaqus. The same columns which were calculated in the previous chapter will now be modeled and the results will be compared with the ones obtained from the analytic analysis.

6.1 Plain concrete column

The static scheme of the column is seen in Figure 6.1. In Abaqus the model is created with the same boundary conditions as the analytic model in order for the results to be accurate.

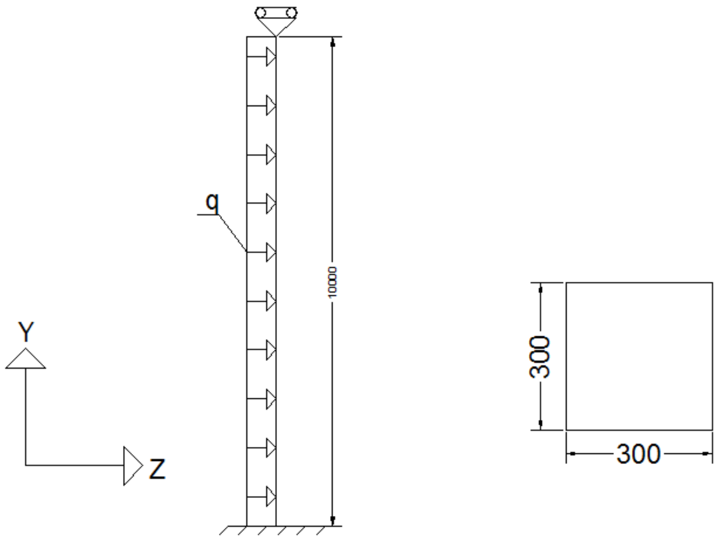

Figure 6.1. Static scheme and cross-section of column.

6.1.1 Materials

As in the case with the beam, concrete is defined in Abaqus with a Young's modulus of 30 000 N/mm^2 and a Poisson's ratio of 0.2, with a compression strength of 20 N/mm^2 and tensile strength of 1.5 N/mm^2. Materials are presented in Chapter 2.

6.1.2 Analysis

In order to run the analysis other parameters have to be defined. The analysis assumes that the concrete behavior is linear-elastic so the properties regarding plasticity, the compression strength and the tensile strength, are not taken into account.

Boundary conditions

The boundary conditions are set to be the same as the analytic model in order to get results which can be compared. The static scheme used to model the boundary conditions is seen in Figure 6.1.

Loading

Because Abaqus will infinetly compress the column during its analysis a very small uniformly distributed lateral load q is added on the Z direction to start the instability process. In order to see the influence of the lateral on the critical buckling load of the column, four models with different lateral loading have been analyzed. The lateral loads applied are $0.01\,\mathrm{N/mm^2}$, $0.001\,\mathrm{N/mm^2}$, $0.0001\,\mathrm{N/mm^2}$ and $0.000\,01\,\mathrm{N/mm^2}$.

In order to get more accurate results, instead of loading the column with a load, a displacement of 100 mm is forced on Y direction along the column length.

6.1.3 Meshing

Knowing, from the beam analysis, the fact that an 8 node hex element is the quickest and also gives good results, this type of element is used in order to mesh the model. The mesh of the model is seen in Figure 6.2

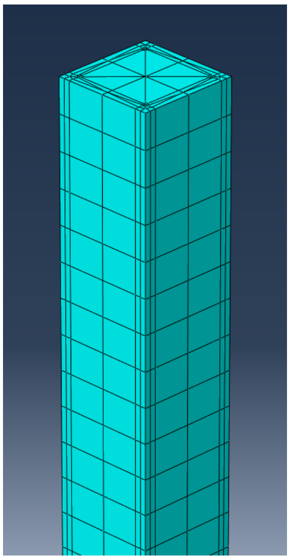

Figure 6.2. Boundary condition at the bottom of the column.

Convergence analysis

A convergence analysis is performed the same way as in Chapter 4 in order to find a balance between accuracy of results and computational pwer. The critical buckling loads calculated for the same lateral load of 0.01 N/mm^2 are compared for different types of meshes. The results are seen in Table 6.1 and presented as graph in Figure 6.3.

Table 6.1. Critical buckling load for different meshes.

Mesh size mm	Number of degrees of freedom	Critical buckling load $[N \cdot 10^6]$	Time [s]
25	1 382 400	1.765	782
50	172 800	1.762	43
75	51 072	1.760	27
100	38 400	1.763	20
125	7680	1.400	11
150	6432	1.402	11
175	5472	1.402	10
200	4800	1.412	10

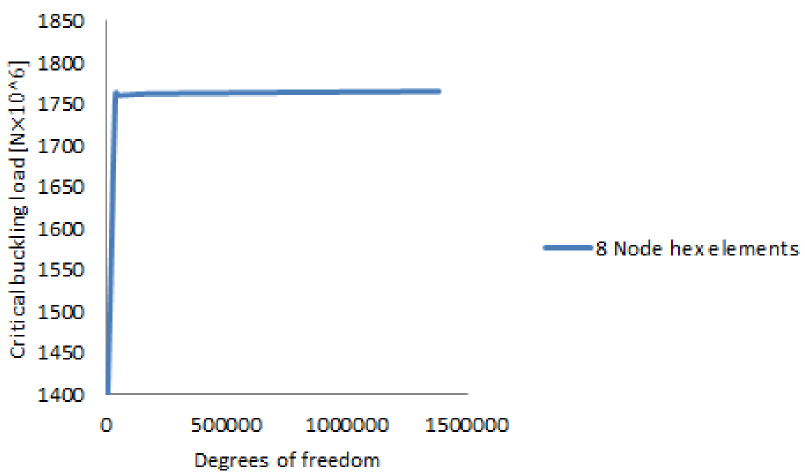

Figure 6.3. Critical buckling loads for different meshes.

From the results it is seen that the critical buckling load doesn't differ much with the increase of the number of degrees of freedom. The big difference between a mesh size of 100 mm and 125 mm is due to the way the column cross-section is meshed as seen in Figure 6.4

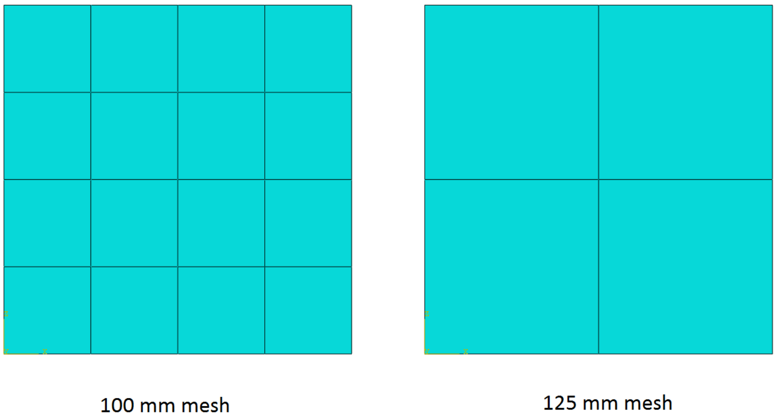

Figure 6.4. Meshing of the column cross-section.

From the mesh size of 25 mm and 100 mm the critical buckling length is closer to the analytic one. The best mesh as computational power and accuracy of the results is the one with a mesh size of 100 mm so the next models will have this mesh size.

6.1.4 Results

After the analysis is done the obtained critical loads obtained are compared with the one in the analytic analysis. The deformed shape is seen in Figure 6.5. It is observed that the deformed shape matches the one from the analytic analysis, seen in case "e" from Figure 5.2.

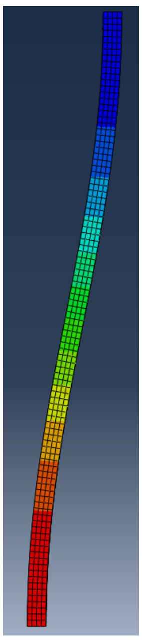

Figure 6.5. Deformed shape of the column.

A plot of the analysis results is presented in Figure 6.6. The results are seen in Table 6.2.

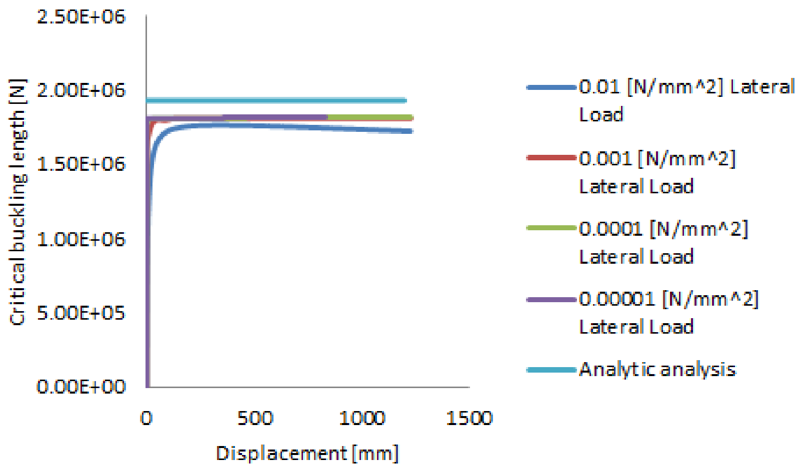

Figure 6.6. Force-displacement diagram for different lateral loads.

The critical buckling load is chosen from the analysis when the graph becomes a stable line, which shows that the column failed due to instability.

Table 6.2. Load bearing capacity of different approaches.

Type of analysis	Critical buckling load $[\mathrm{N} \cdot 10^6]$
Lateral Load $0.01\,\mathrm{N/mm^2}$	1.763
Lateral Load $0.001\,\mathrm{N/mm^2}$	1.803
Lateral Load $0.0001\,\mathrm{N/mm^2}$	1.813
Lateral Load $0.000\,01\,\mathrm{N/mm^2}$	1.815
Analytic Analysis	1.932

From the table it is observed that the critical buckling load of the column acted with the largest lateral load and the smallest lateral load is 3 %. Also from the results it is seen that there is a 6 % difference between the critical buckling load calculated with the analytic method and the critical buckling load from the analysis with a lateral load of $0.000\,01\,\mathrm{N/mm^2}$.

The results are presented in the form of a graph which is seen in Figure 6.7

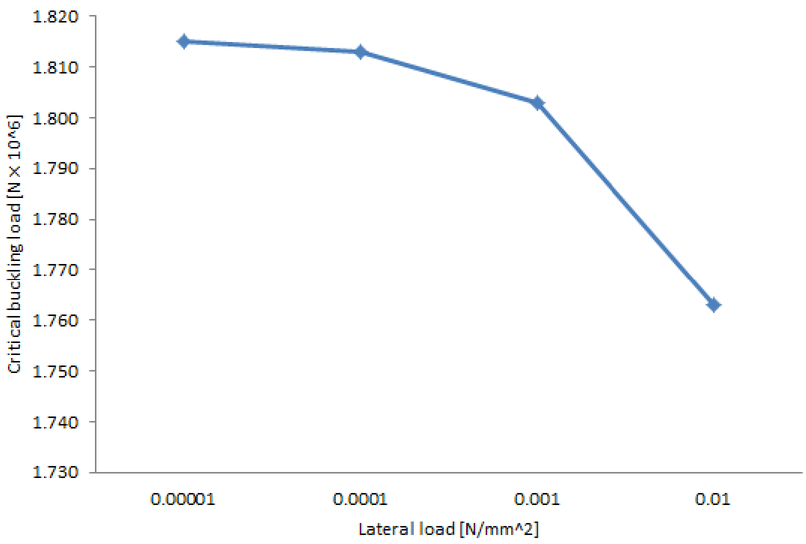

Figure 6.7. The critical buckling load in function of the lateral load.

From the figure it is observed that critical buckling load increases as the lateral load decreases.

6.1.5 Plasticity

The same analysis is run as before only this time plasticity is added to the concrete and all the concrete properties mentioned before are taken into account, which means that the concrete acts non-linear.

Results

Again, four models are tested in order to see the influence of the eccentricity. A plot of the results is presented in Figure 6.8. The results are seen in Table 6.3.

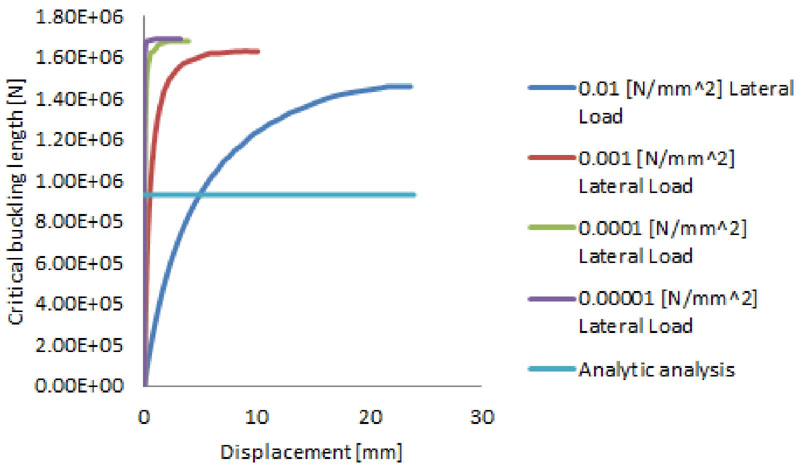

Figure 6.8. Force-displacement diagram for different lateral loads.

Table 6.3. Load bearing capacity of different approaches.

Type of analysis	Critical buckling load $[N \cdot 10^6]$
Lateral Load $0.01\,N/mm^2$	1.461
Lateral Load $0.001\,N/mm^2$	1.634
Lateral Load $0.0001\,N/mm^2$	1.643
Lateral Load $0.000\,01\,N/mm^2$	1.685
Analytic Analysis	0.931

From the results it is seen that the difference of the obtained critical buckling load from the model with a lateral load of $0.01\,N/mm^2$ and then one with a lateral load of $0.000\,01\,N/mm^2$ is 13 %. From all the results it is seen that the model with a lateral load of $0.000\,01\,N/mm^2$ is the closest simulation of a buckling failure. Also the analytic solution is very conservative in comparison with the numerical solution.

The results are presented in the form of a graph which is seen in Figure 6.9.

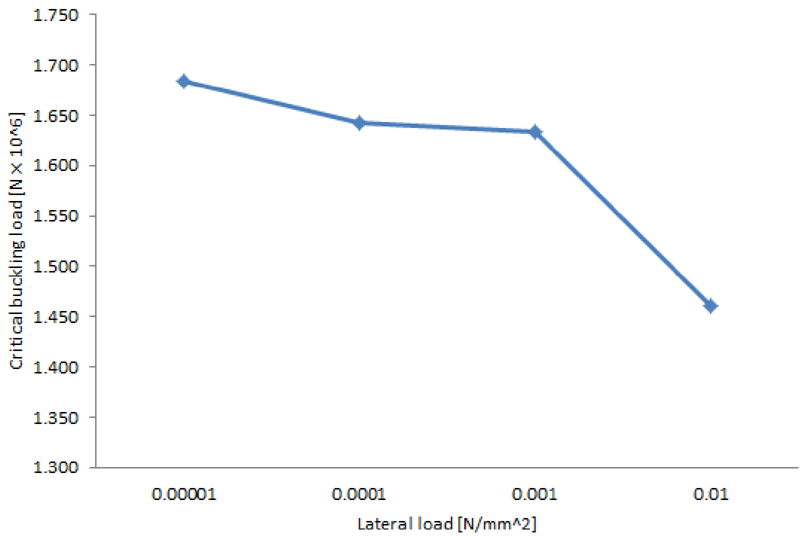

Figure 6.9. The critical buckling load in function of the lateral load.

From the figure it is observed that critical buckling load increases as the lateral load decreases.

6.2 Reinforced concrete column

To increase the critical buckling load, reinforcement is added to the concrete cross-section as seen in Figure 6.10.

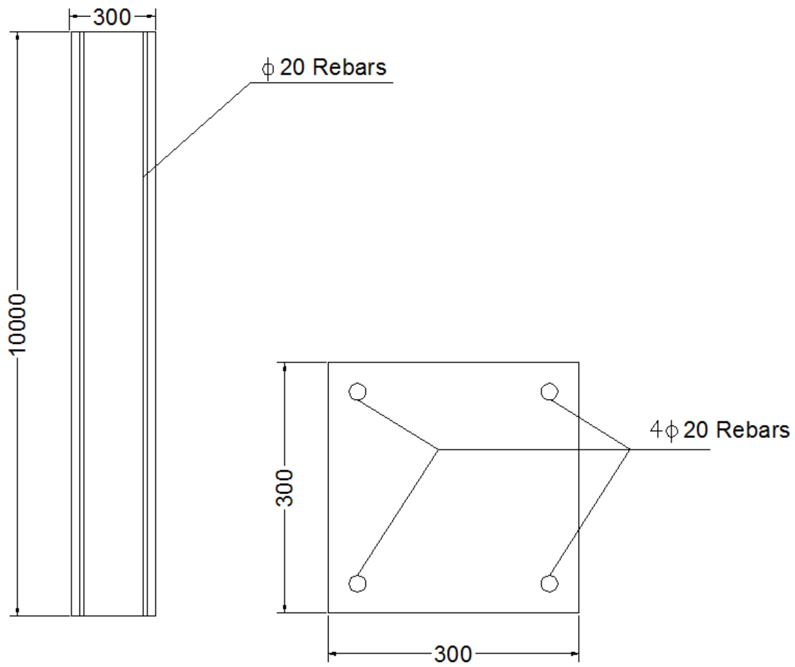

Figure 6.10. Reinforced concrete cross-section.

6.2.1 Column model

Even though in Chapter 4, it is shown that modeling the reinforcement as wire elements is the fastest way to run the analysis, for the case of column, due to the non-linearity taken into account, the models won't work, so the reinforcement is modeled as solid.

6.2.2 Materials

The materials are defined the same as in the analysis done in chapter 4.

6.2.3 Analysis

The analysis is done the same way as before with the previous models.

6.2.4 Boundary Conditions

The boundary conditions are the same as the homogeneous column, being fixed at the bottom and restricting displacement on Y direction at the top.

6.2.5 Loading

The loading is done in the same way as with the homogeneous column. There are also four models analyzed with different lateral loading in order to see its effect.

6.2.6 Meshing

The meshing is done with 8 node hex elements as in the previous analysis.

6.2.7 Results

The obtained critical buckling after finishing the analysis is compared with the previous obtained results and with the analytic results. This is done to see how much of an improvement the reinforcement has on the critical buckling load.A plot of the results is presented in Figure 6.11. The results are seen in Table 6.4.

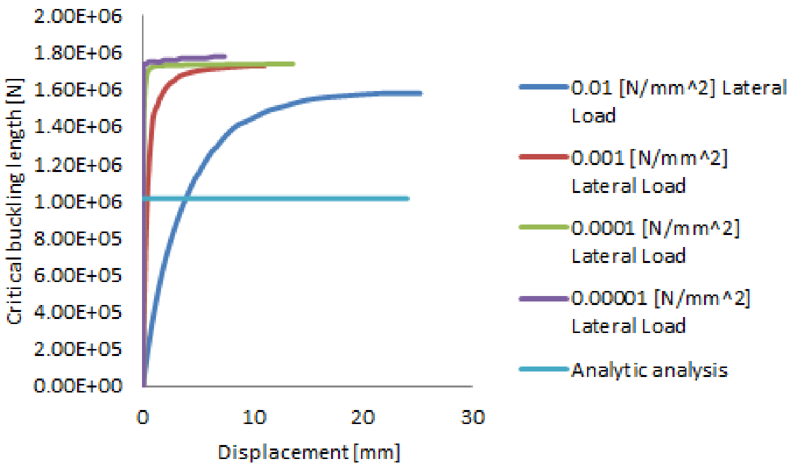

Figure 6.11. Force-displacement diagram for different lateral loads.

Table 6.4. Load bearing capacity of different approaches.

Type of analysis	Critical buckling load $[\mathrm{N} \cdot 10^6]$
Lateral Load $0.01\,\mathrm{N/mm^2}$	1.580
Lateral Load $0.001\,\mathrm{N/mm^2}$	1.729
Lateral Load $0.0001\,\mathrm{N/mm^2}$	1.743
Lateral Load $0.000\,01\,\mathrm{N/mm^2}$	1.776
Analytic Analysis	1.013

From the table it is observed that the difference in critical buckling load between the model with a lateral load of $0.01\,\mathrm{N/mm^2}$ and the one with a lateral load of $0.000\,01\,\mathrm{N/mm^2}$ is 11 % .

The results are presented in the form of a graph which is seen in Figure 6.12

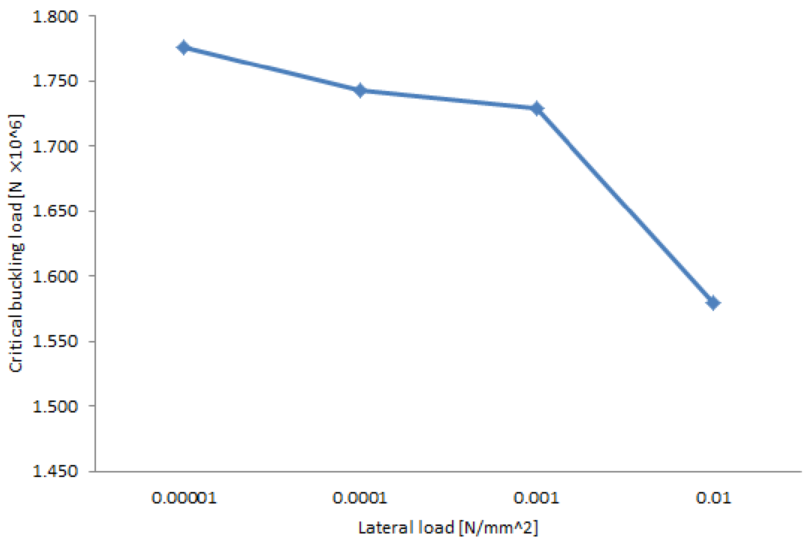

Figure 6.12. The critical buckling load in function of the lateral load.

From the figure it is observed that critical buckling load decreases as the lateral load increases.

6.3 Influence of stirrups

After the analysis of the reinforced concrete column, stirrups are added along the column length in order to see their influence on the critical buckling load. The stirrups are also modeled as solid elements, the same as the longitudinal reinforcement, with a diameter of 8 mm. Six models are created with a distance of 100 mm, 200 mm, 300 mm, 400 mm and 500 mm, 1000 mm between the stirrups. Even though the closest model to a centrally loaded column is the one with a lateral load of 0.000 01 N/mm^2 it requires large computational power to run the analysis so the lateral load chosen is 0.0001 N/mm^2. The column cross-section and the longitudinal reinforcement are considered merged as one piece in the model and the stirrups are considered to be embedded inside the column. In Figure 6.13 it is seen the cross-section of the column with the stirrups.

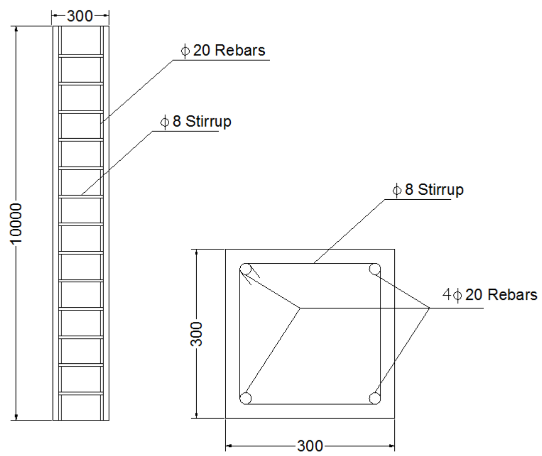

Figure 6.13. Cross-section of the column with stirrups.

6.3.1 Analysis

Six models are analyzed with the same parameters the only difference between them being the number of stirrups and distance between them. Initially only three models were used but because of observing no trend in the results, three more models were analyzed. The force-displacement diagrams for the models are shows in Figure 6.14. The results are presented in Table 6.5.

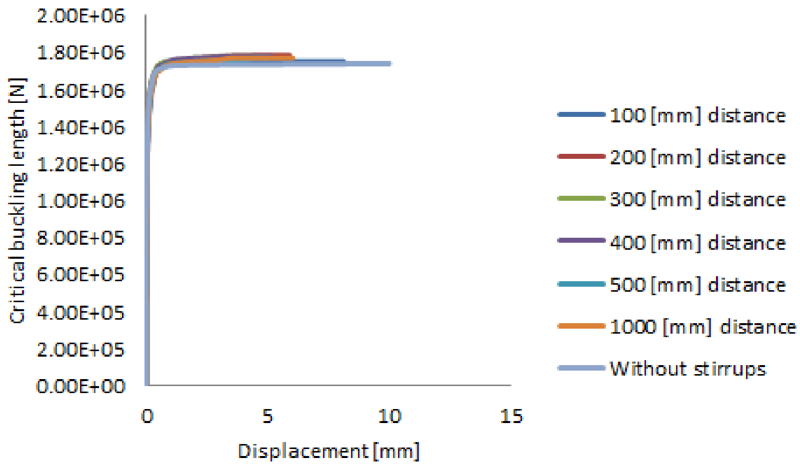

Figure 6.14. Force-displacement diagrams for models with different distance between stirrups.

Table 6.5. Critical buckling load for different models.

Distance between stirrups [mm]	Number of stirrups	Critical buckling load $[\mathrm{N} \cdot 10^6]$
100	100	1.752
200	50	1.784
300	34	1.780
400	25	1.783
500	20	1.765
1000	10	1.773

From Figure 6.14, it is observed that the distance between stirrups makes a difference of 3% between the highest obtained critical buckling and the lowest obtained critical buckling load.

In order to observe the results better, they are plotted in a graph. The graph is seen in Figure 6.15.

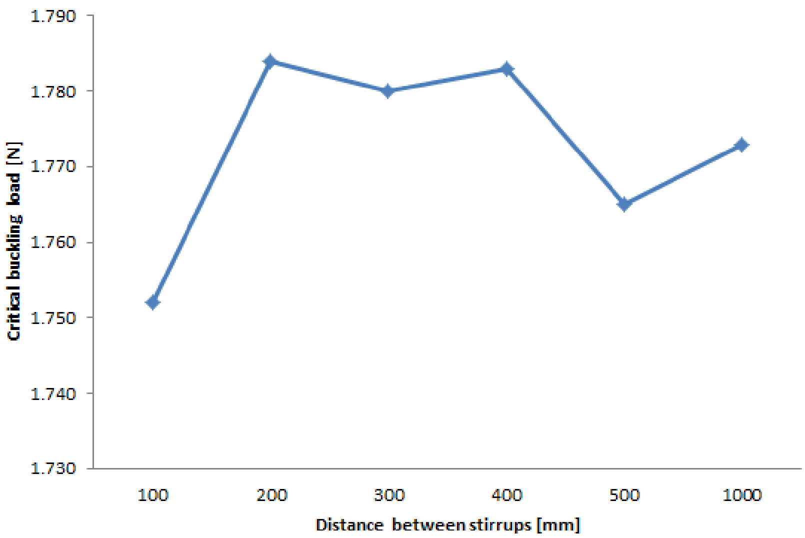

Figure 6.15. Critical buckling load with different distance between stirrups.

From the graph it is observed that there is no particular trend in the increasing or decreasing of the critical buckling depending on the distance between stirrups. The highest critical buckling load is obtained when the distance between stirrups is 200 mm.

The critical buckling loads of all the analytic analyses and numerical analyses of the models with a lateral load of $0.0001\,\mathrm{N/mm^2}$ are presented in Figure 6.16 and Table 6.6.

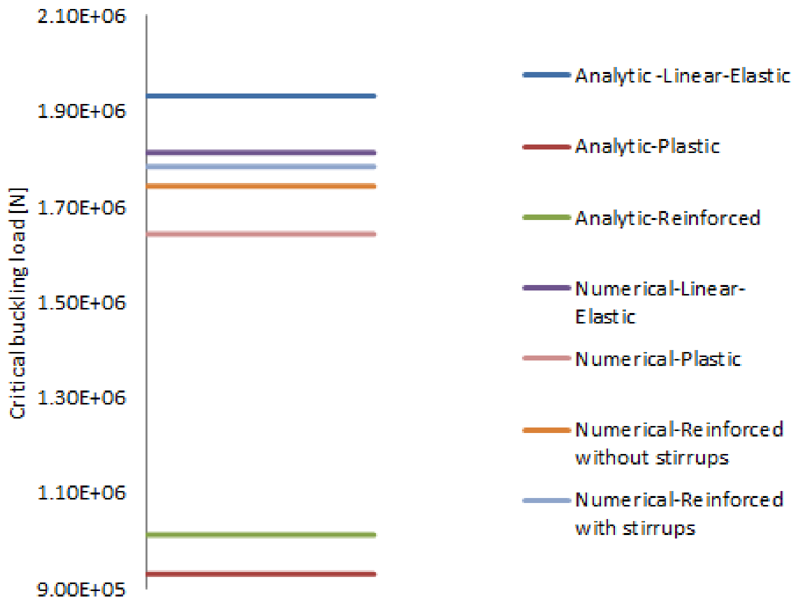

Figure 6.16. Critical buckling load with different analyses.

Table 6.6. Critical buckling load for different models.

Type of analysis	Elastic	Plastic	Reinforced without stirrups	Reinforced with stirrups
Analytic	1.932	0.931	1.013	-
Numeric	1.813	1.643	1.743	1.784

From Figure 6.16 it is observed that the highest critical buckling load is obtained with the analytic linear elastic approach and the lowest critical buckling load with the analytic plastic approach the difference between them being 52%. From the numerical analysis it is also observed that the difference between the critical buckling load of a plain concrete column and a reinforced one is 10% and the addition of stirrups raises the critical buckling load by an additional 3%.

Conclusion 7

In order to design reinforced concrete structure, along the years analytic solutions were developed in order to assist the designer and also to ensure safety of the population using these buildings as workplaces or homes, etc. Now with the help of modern technology 3D finite element analysis software are starting to be used in designing of structures, which even though require understanding of the software itself, it brings more accurate results, closer to real life situations than the analytic solutions. The purpose of this report is too compare the results of two type of analyses, numerical and analytical, for two different structural elements, beams and columns.

In order to be sure the physical phenomenons are understood gradually more complex elements are analyzed. The bearing capacity and maximum displacement of a plain concrete beam is calculated with the assumption that the concrete acts linear-elastic.

Because in most real-life structures reinforcement is used in order to increase the bearing capacity of the beam, the same is done in the report. As in real life conditions when adding reinforcement to the concrete beam, it's bearing capacity and maximum displacement allowed are increased.

Numerical analysis with Abqaqus software is performed with the exact same steps as in the analytic model. Because of the challenges of modeling concrete in Abaqus, the beam is modeled with increasingly complex materials, in order to make sure that the models provide good results. Initially a linear-elastic material is used to model the beam and the results obtained from the analysis is compared with the analytic results. The difference between the results is very small so it is shown that the model is created correctly. After that plasticity is added to the material in order to simulate concrete and a load bearing capacity is calculated.

Reinforcement is added to the model with the same dimensions and properties as in the analytic analysis and it is observed that the bearing capacity is increased in comparison with the model without reinforcement which shows that the model is created correctly. The presence of the reinforcement greatly increases the load bearing capacity of the beam.

The effect of stirrups is investigated in order to see how it affects the bearing capacity of the reinforced concrete beam. Ten models with different lengths are analyzed. It is observed that as the length of the beam increases, the influence of the stirrups decreases, this is due to the shear force having a higher influence in short beams and bending moment in long beams.

[EN 1992-1-1, 2014] shows the possibility of using bent rebars. Their influence is investigated and it is observed that they increase the bearing capacity even more than the straight rebars or the stirrups. This is due to the increase in reinforcement area.

An analytic analysis of the critical buckling length of a centrally loaded column is performed. Initially it is assumed that the concrete act linear-elastic and after this it is assumed that it acts non-linear. It is observed a 50 % difference between the two approaches in the calculation of the critical buckling load. This is due to the fact that the formula used for the plastic approach is very conservative.

A reinforced concrete column is analyzed in order to see how the reinforcement affects the critical buckling load. The reinforcement has a small influence on the critical buckling load this is because the area of the reinforcement rebars is small compared to that of the concrete cross-section.

A numerical model is created in order to compare the results with the analytic solution. The material is modeled with increased complexity as with the case of the beam. As Abaqus would compress the column indefinitely a lateral load is applied on a lateral surface of the column in order to start the instability process. Analyses with different lateral loads are performed and it is observed that the lateral has a small impact on the critical buckling load of the column modeled with a liner-elastic concrete and a higher impact on the critical buckling load modeled with a non-linear concrete. The difference between the critical buckling load obtained from numerical analysis and analytic analysis is small in case of linear-elastic concrete, but the difference is high in case of non-linear concrete.

Reinforcement is added to the column model and it is observed that the critical buckling load increases.

In order to see the influence of stirrups, six models are created with different distance between the stirrups. No particular trend is observed in increasing or decreasing the critical buckling load with different distances between stirrups, but the highest critical buckling load is obtained when the distance between stirrups is 200 mm.

Bibliography

Agent, 2008. Radu Agent. *Behavior and calculation of reinforced concrete elements.* DHI, 2008.

Autodesk, 2015. *Autodesk.* URL: `http://sustainabilityworkshop.autodesk.com/products/metrics-and-basics-mechanics`, 2015.

EN 1992-1-1, 2014. EN 1992-1-1. *Eurocode 2: Design of concrete structures.* ISBN: 978-87-7310-572-6, 1. udgave, 1. oplag. European Committee for Standardisation, 2014.

MIT, 2014. MIT. *Tetahedron elements.* URL: `http://web.mit.edu/calculix_v2.7/CalculiX/ccx_2.7/doc/ccx/node25.html`, 2014. Downloaded: 03-12-2015.

Simulia, 2016. BS Simulia. *Abaqus 6.13 - Abaqus/CAE User's Manual.* BS Simulia, 2016.